Structures 62 (2024) 106153

Contents lists available at ScienceDirect

Structures

journal homepage: www.elsevier.com/locate/structures

Prevention of brittle failure for steel connections utilizing special devices

Salvatore Benfratello *, Luigi Palizzolo

Department of Engineering, University of Palermo, Italy

ARTICLE INFO

Keywords:
Steel structures
Steel connections
LRPD
Optimal design
Welding protection
Brittle failure

ABSTRACT

The present paper proposes the use of a special design procedure devoted to the prevention of brittle failure for welded steel connections. In particular, reference is made to steel frame structures made up of beam elements with I-shaped cross-sections where the connections between columns and beams are usually welded and/or bolted. The proposed new design procedure consists of four subsequent analysis steps; it is based on the identification and analytical definition of new appropriate brittle safe domains defined in the N, V, M space and on the use of suitably designed devices (LRPD), recently proposed by the authors, belonging to the class of the RBS connections. The latter are able to impose prefixed values of internal forces on selected beam element cross-sections, avoiding any modification of the elastic stiffness features of the involved beam. The main novelties of the present study consist in the introduction of new brittle safe domains for I-shaped cross-sections, in the specialization of the LRPD optimal design to the present context and in the definition of a special design strategy which allows to contextually obtain structures safe from the risk of brittle failure as well as being able to dissipate an appropriate amount of plastic strain energy. The numerical application, devoted to plane steel frames, confirms the sound reliability of the procedure and the great flexibility of the utilized LRPDs.

1. Introduction

In the framework of steel structures, connections between beams and columns are the most critical portions to be investigated. The European code of design [1] proposes the classification of the structural steel connections both in terms of stiffness, identifying three different types of connections (rigid, semi-rigid and nominally pinned), and in terms of strength, identifying three alternative types of connections (full strength, partial strength and, again, nominally pinned). As is common knowledge, steel structures perform best when their ductility features are appropriately used; in this case the structure design must be based on appropriate elastic plastic analyses and such occurrence makes relevant the above described strength classification. For the purposes of the present paper, moment resisting connections will be considered, representing appropriate rigid and full-strength connections.

The relevant beam-column connection is usually achieved by welding steel plates at the ends of the beam and bolting them to the flange columns in the panel zone, so that the adoption of welding is unavoidable. The main role of a structural connection is force transmission between the connected sections and, therefore, this connection should possess clearly describable mechanical properties, suitably high ultimate load capacity and pronounced ductility [2]. All these requisites, for given geometry, depend both on the mechanical properties of the base material and on the welding technological process. Unfortunately, as is well known, welding produces a modification of the material crystal lattice and, consequently, the transition from the desired ductile behaviour to an undesired brittle one. Therefore, it is precautionary to make suitable elastic checks for the welded connections, adopting appropriate safety factors to avoid any dangerous brittle collapse. This problem is particularly relevant when the seismic design of steel structure is carried out, as was demonstrated by the 1994 Northridge and 1995 Kobe earthquakes which produced devastating effects on structural steel connections, highlighting failure phenomena due to brittle behaviour. The consequent structural collapse gave rise to many studies (see e.g. [3,4]) on steel connections.

Therefore, one of the main matters to be faced is the definition of a good strategy to design steel structures which at the same time fulfil safety with regards to the possible brittle failure and exhibit good ductile behaviour. Current Italian standards for constructions [5], in alignment with Eurocode 8 prescriptions [6], aim for the application of the well-known and consolidated capacity design approach for new buildings in seismic-prone areas. In accordance with this approach, selected elements of the structures are devoted to the development of plastic deformations to maximize the dissipation of the energy stored during

* Correspondence to: Department of Engineering, University of Palermo, Viale delle Scienze, Building 8, 90144 Palermo.
E-mail address: salvatore.benfratello@unipa.it (S. Benfratello).

https://doi.org/10.1016/j.istruc.2024.106153
Received 9 August 2023; Received in revised form 17 February 2024; Accepted 29 February 2024
Available online 14 March 2024

seismic events and to achieve a global ductile collapse mechanism. Many different typologies of structural elements, as concentrically and not concentrically braces [7,8], RBS (see e.g. [9–11]), dissipative connections (see e.g. [12–14]), are available to the designer to achieve the above-described goal, but they do not deal with the undesired brittle behaviour.

A recommended strategy within the framework of RBS connections, utilized in the present paper, consists of limiting the stresses acting on the beams' end sections realising the welded connection (in the following synthetically referred to as BWC) by making use of special innovative devices for beam-column connections named Limited Resistance Plastic Device (LRPD), already proposed by the authors [15–22]. As widely reported in [21,22], the LRPD possesses the property of suitably reducing the generalized stresses at the beam extreme maintaining unaltered the elastic bending stiffness and ensuring the production of the expected amount of plastic dissipation. These latter features make the described device different from the usual adopted ones, available for structural designers [23–26] and approved by international codes (see e.g. [27–29]).

The main aim of the present paper is to give a response to the previously introduced matter by defining appropriate new reduced elastic domains (brittle safe) for the typical I-shaped steel cross-section based on the Von Mises criterion. The paper proposes a new design strategy for flexural steel frames able to obtain structures safe with respect to any brittle failure risk and, furthermore, able to exhibit resistance capacity beyond their elastic limit and to dissipate an appropriate amount of plastic strain energy.

The proposed design procedure will be performed in four consecutive steps: i) a classical standard code design is obtained by performing a modal analysis referring to the relevant response spectrum; ii) the real behaviour of the structure so designed is checked by performing a step by step elastic plastic dynamic analysis with the aim of identifying the BWC where the elastic plastic behaviour is required; iii) on the ground of the defined new reduced elastic domain (brittle safe) of the relevant cross-sections, defined in a suitable analytic form and represented in the N, V, M space, the limit value of the relevant bending moment to be imposed at the selected cross-sections for ensuring a safe brittle behaviour is determined; iv) the optimal LRPDs to be placed at the end of the beams, which ensure the fulfilling of the previously defined safe condition, are obtained by solving suitably formulated optimal design problems.

In the following, at first the brittle safe domains for I-shaped steel cross-sections will be defined utilizing a discrete linearized procedure; subsequently, a new version of the optimal design for LRPDs will be proposed, specialized to the present case in order to ensure the prevention of dangerous brittle failure and the virtuous utilization of the ductility characteristic of the structure; furthermore, the proposed design procedure will be explicitly described and applied to a two span and two floors plane steel frame. Finally, a useful comparison between the LRPDs and the most utilised RBS connections (dogbone) will be examined. All the obtained results confirm the full reliability of the procedure and the efficacy of the new optimal design approach.

2. Definition of the brittle safe domain

Making reference to Fig. 1, a typical I-shaped cross-section of a steel beam element is considered; limiting the interest to plane frame structures, the behaviour of the considered cross-section depends on the simultaneous presence of axial force N, shear force $V \equiv V_z$ along one of the inertia central axes and bending moment $M \equiv M_y$.

The analysis of the behaviour of steel cross-sections subjected to the simultaneous action of axial force, shear force and bending moment has already been looked at in several studies (see, e.g. [30,31]), while it is not sufficiently investigated in the international standard rules [1,5,8]; in particular, in [30] and [31] the effect of the three generalised stresses is studied for I-shaped sections, double channel sections and hollow

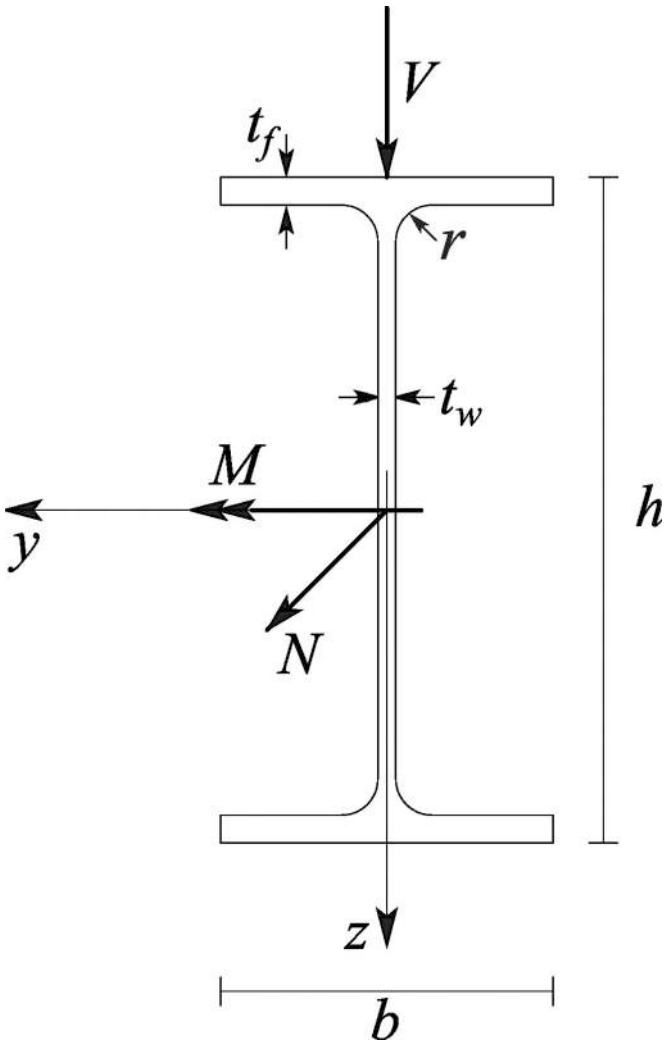

Fig. 1. Typical I-shaped cross-section under examination.

rectangular sections appertaining to Class 1, 2 and 3, providing very useful formulation for practical applications, but always referring to the ultimate strength of the relevant sections and usually adopting a simplified model which takes into account the combined effect of the acting stresses. If the limit state to avoid in BWC is related to the risk of brittle failure, in these sections an elastic behaviour with suitable safety factors must be required. Therefore, in the following some specific reduced elastic domains (brittle safe) are analitically defined for I-shaped steel cross-sections to be utilized for the design of connections able to ensure suitable safety factors against brittle failure.

For the construction of the specific reduced elastic domains, reference will be made to the classical normal and shear stress distributions characterizing the local response related to the axial force N, the shear force V and the bending moment M.

Making reference to Fig. 2, indicating with A and I_y the area of the cross-section and the related moment of inertia with respect to the y axis, in each point the normal stress is the algebraical sum of the one involved by the axial force $(\sigma_x = N/A)$ and the one due to the bending moment $\left[\sigma_x(z) = \left(M/I_y\right)z\right]$, suitably condensed in a single linear diagram, while the diagram of the shear stress along the flange $\tau_{xy} = \frac{V \bullet S_y^{A_z}}{I_y \bullet t_f}$ and that along the web $\tau_{xz} = \frac{V \bullet S_y^{A_y}}{I_y \bullet t_w}$ are sketched with reference to the medium lines of flange and web, respectively, and reported in Fig. 3, where $S_y^{A_z}$ and $S_y^{A_y}$ indicate the first order moments of the area subtended by a chord parallel to z and y axes, respectively, evaluated with respect to the

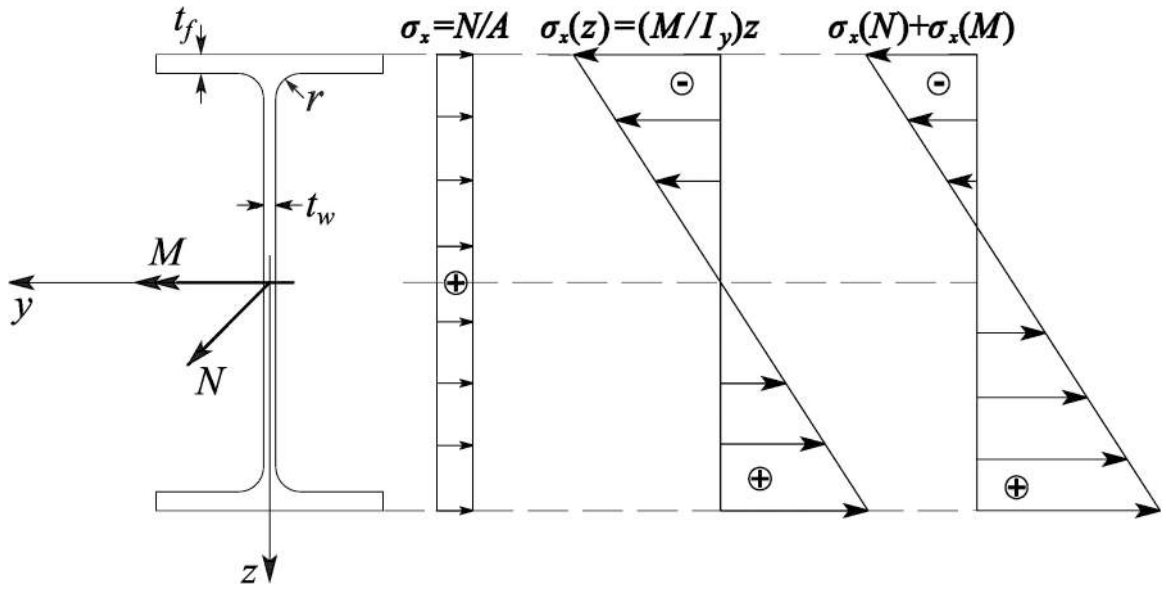

Fig. 2. Stress distribution for axial force and bending moment.

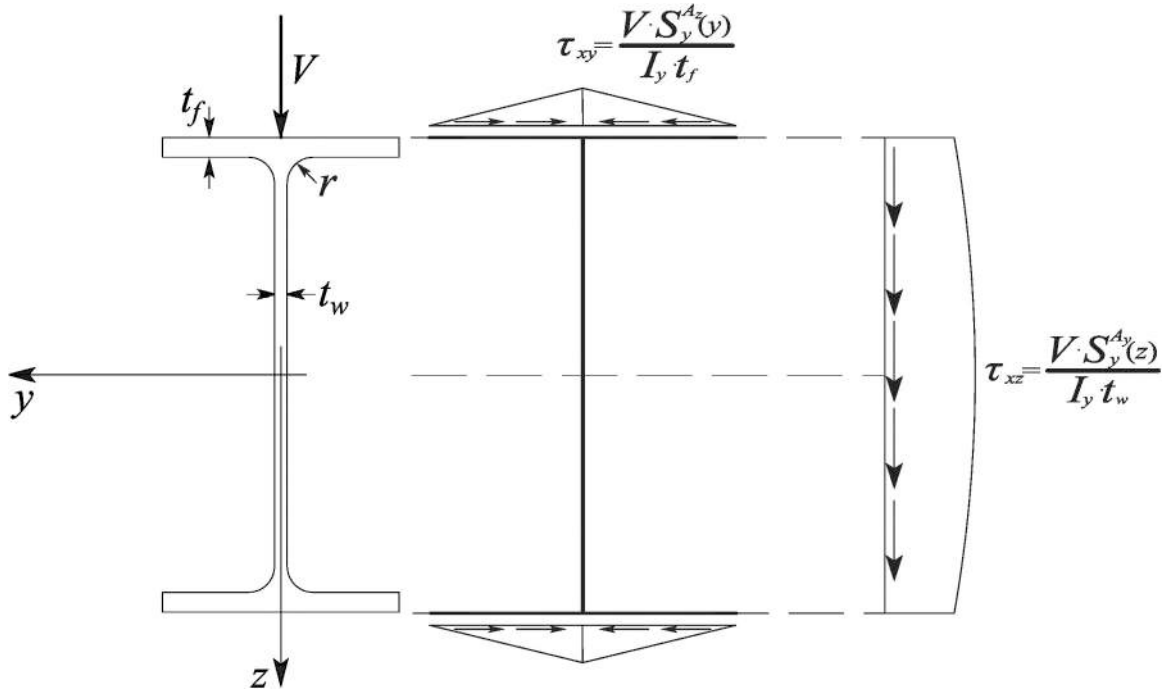

Fig. 3. Stress distribution for shear force.

barycentric y axis.

According to the Von Mises criterion and indicating with σ_b the reduced brittle limit stress, in each point of the relevant cross-section the significant limit condition holds:

$$\sqrt{\sigma_x^2+3\left(\tau_{xy}^2+\tau_{xz}^2\right)}=\sigma_b \tag{1}$$

In Eq. (1) $\sigma_b=\sigma_0/\gamma_b$, with σ_0 material yield stress and $\gamma_b=1.25$ an appropriately chosen safety factor against the brittle failiure (see Table 4.2. XIV of [5]). In particular, at extrados and intrados of the relevant I-shaped cross-section, the condition reads:

$$\sqrt{\sigma_x^2+3\tau_{xy}^2}=\sigma_b \Longrightarrow \sigma_x^2+3\tau_{xy}^2=\sigma_b^2 \tag{2}$$

and within the web the condition reads

$$\sqrt{\sigma_x^2+3\tau_{xz}^2}=\sigma_b \Longrightarrow \sigma_x^2+3\tau_{xz}^2=\sigma_b^2 \tag{3}$$

Moreover, it results:

- pure axial force
  $\sigma_x=\sigma_{x,\max}=\frac{N}{A}$ in any point of the cross-section and $N_b=A\sigma_b$, being N_b the limit brittle safe axial force;
- pure bending moment
  $\sigma_{x,\max}=\frac{M}{W_y^E}$ at extrados or intrados (depending on the sign of M) and $M_b=W_y^E\sigma_b$, being M_b the limit brittle safe bending moment and W_y^E the elastic resistance modulus of the cross-section;

- pure shear force

  $\tau_{xy,\max} = \frac{V \bullet S_y^{A_z}\left(\frac{b}{2}\right)}{I_y \bullet t_f}$ at extrados or intrados and in absence of τ_{xz}, $\tau_{xz,\max} = \frac{V \bullet S_y^{A_y}(G)}{I_y \bullet t_w}$ in correspondence of the cross-section centre of gravity and in absence of τ_{xy},

  $\tau_{xz,\max} > \tau_{xy,\max}$ always results and $V_b = \frac{\tau_b \bullet I_y \bullet t_w}{S_y^{A_y}(G)}$, being V_b the limit brittle safe shear force with $\tau_b = \sigma_b/\sqrt{3}$ the reduced brittle limit shear stress.

2.1. Domain boundary on N, M plane

Considering the cross-section subjected just to axial force and bending moment, on the first quarter of the N, M plane, the maximum value of the normal stress at the cross-section intrados holds:

$$\sigma_{x,\max}(N,M) = \frac{N}{A} + \frac{M}{W_y^E} \text{ with } \tau_{xy} = \tau_{xz} = 0 \text{ at any point} \tag{4}$$

Therefore, the cross-section domain boundary on the first quarter of the N, M plane, $\forall N \in (0; N_b), \forall M \in (0; M_b)$, is defined by the function:

$$\sqrt{\sigma_{x,\max}^2} = \sigma_b \tag{5}$$

i.e.

$$\sqrt{\left(\frac{N}{A} + \frac{M}{W_y^E}\right)^2} = \sigma_b \tag{6}$$

and finally:

$$\frac{N}{A} + \frac{M}{W_y^E} = \sigma_b \tag{7}$$

On the other quarters of the N, M plane, the boundary can be defined imposing symmetry with respect to the N and M axes. In Fig. 4 the reduced elastic domain (brittle safe) is reported in the plane N, M referring to a IPE360 S235 steel profile whose basic dimensions and geometrical properties are reported in Table 1.

2.2. Domain boundary on N, V plane

Considering the cross-section subjected just to axial and shear forces, on the first quarter of the N, V plane, the maximum value of the normal stress and of the shear stress are in correspondence to the center of gravity and they hold:

Table 1
Dimensions and geometrical properties of the IPE360 profile.

Adopted Symbol	Value
Section width b	170 mm
Section depth h	360 mm
Web thickness t_w	8 mm
Flange thickness t_f	12.7 mm
Root radius r	18 mm
Area A	7273 mm^2
Elastic resistance modulus $W_{el,y}$	903,600 mm^3
Plastic resistance modulus $W_{pl,y}$	1019,000 mm^3
Moment of inertia I_y	162,700,000 mm^4

$$\sigma_x(N) = \frac{N}{A} \tag{8}$$

and

$$\tau_{xz,\max} = \frac{V \bullet S_y^{A_y}(G)}{I_y \bullet t_w} \tag{9}$$

Therefore, the cross-section domain boundary on the first quarter of the V, N plane, $\forall N \in (0; N_b), \forall V \in (0; V_b)$, is defined by the function:

$$\sqrt{\sigma_x^2 + 3\tau_{xz,\max}^2} = \sigma_b \tag{10}$$

i.e.

$$\sqrt{\left(\frac{N}{A}\right)^2 + 3\left(\frac{V \bullet S_y^{A_y}(G)}{I_y \bullet t_w}\right)^2} = \sigma_b \tag{11}$$

and finally:

$$\left(\frac{N}{A}\right)^2 + 3\left(\frac{V \bullet S_y^{A_y}(G)}{I_y \bullet t_w}\right)^2 = \sigma_b^2 \tag{12}$$

On the other quarters of the N, V plane, the boundary can be defined imposing symmetry with respect to the N and V axes. In Fig. 5 the reduced elastic domain (brittle safe) is reported in the plane N, V always referring to a IPE360 S235 steel profile.

2.3. Domain boundary on M, V plane

Considering the cross-section subjected just to shear force and bending moment, on the first quarter of the M, V plane, the maximum value of the normal stress and that of the shear stress along the y axis find themselves in correspondence of the medium point of the section intrados and they hold:

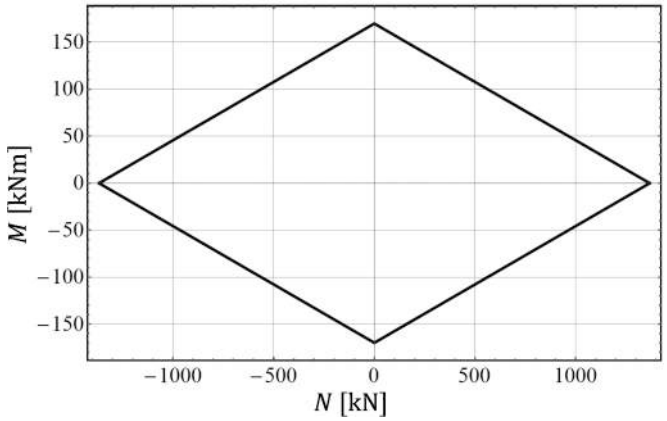

Fig. 4. Reduced elastic domain in N, M plane for IPE360 S235 steel profile.

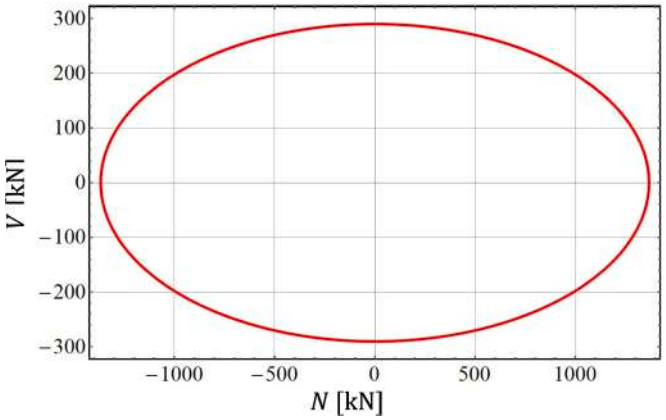

Fig. 5. Reduced elastic domain in N, V plane for IPE360 S235 steel profile.

$$\sigma_{x,\max}(M) = \frac{M}{W_y^E} \tag{13}$$

and

$$\tau_{xy,\max} = \frac{V \bullet S_y^{A_z}\left(\frac{b}{2}\right)}{I_y \bullet t_f} \tag{14}$$

Along the web the normal stress function and the shear force one (along the z axis) read:

$$\sigma_x(M,z) = \frac{M}{I_y} z \tag{15}$$

and

$$\tau_{xz}(V,z) = \frac{V \bullet S_y^{A_y}(z)}{I_y \bullet t_w} \tag{16}$$

Therefore, the cross-section domain boundary on the first quarter of the M,V plane, $\forall V \in (0;V_b), \forall M \in (0;M_b)$, is defined imposing that in correspondence of the medium point of the section intrados the resistance condition is:

$$\sqrt{\sigma_x^2 + 3\tau_{xy,\max}^2} = \sigma_b \tag{17}$$

i.e.

$$\sqrt{\left(\frac{M}{W_y^E}\right)^2 + 3\left(\frac{V \bullet S_y^{A_z}\left(\frac{b}{2}\right)}{I_y \bullet t_f}\right)^2} = \sigma_b \tag{18}$$

and finally

$$\left(\frac{M}{W_y^E}\right)^2 + 3\left(\frac{V \bullet S_y^{A_z}\left(\frac{b}{2}\right)}{I_y \bullet t_f}\right)^2 = \sigma_b^2 \tag{19}$$

and that along the web, $\forall V \in (0;V_b)$, $\forall M \in (0;M_b)$, $\forall z \in \left(0;\frac{h}{2} - t_f\right)$, the resistance condition reads:

$$\sqrt{\sigma_x^2 + 3\tau_{xz}^2} = \sigma_b \tag{20}$$

i.e.

$$\sqrt{\left(\frac{M}{I_y} z\right)^2 + 3\left(\frac{V \bullet S_y^{A_y}(z)}{I_y \bullet t_w}\right)^2} = \sigma_b \tag{21}$$

and finally:

$$\left(\frac{M}{I_y} z\right)^2 + 3\left(\frac{V \bullet S_y^{A_y}(z)}{I_y \bullet t_w}\right)^2 = \sigma_b^2 \tag{22}$$

Therefore, for a sufficiently high number of $\overline{M}$ values ($0 \le \overline{M} \le M_b$), the corresponding limit value of the shear force can be defined as the lower value between

$$V = \left\{ \frac{\left[\sigma_b^2 - \left(\frac{\overline{M}}{W_y^E}\right)^2\right] I_y^2 \bullet t_f^2}{3\left[S_y^{A_z}\left(\frac{b}{2}\right)\right]^2} \right\}^{\frac{1}{2}} \tag{23}$$

and the minimum shear force value obtained by the solution to the following optimization problem:

$$\min_{(z)} V \tag{24a}$$

subjected to

$$0 \le z \le \frac{h}{2} - t_f \tag{24b}$$

$$\left(\frac{\overline{M}}{I_y} z\right)^2 + 3\left[\frac{V \bullet S_y^{A_y}(z)}{I_y \bullet t_w}\right]^2 \ge \sigma_b^2 \tag{24c}$$

On the other quarters of the M,V plane the boundary can be defined imposing symmetry with respect to the M and V axes. In Fig. 6 the reduced elastic domain (brittle safe) is reported in the plane M,V always referring to a IPE360 S235 steel profile.

2.4. Domain boundary surface on the N,V,M space

Considering the cross-section subjected to axial force, shear force and bending moment, on the first octant of the N,V,M space, the maximum value of the normal stress and of the shear stress along the y axis find themselves in correspondence to the medium point of the section intrados and they hold:

$$\sigma_{x,\max}(N,M) = \frac{N}{A} + \frac{M}{W_y^E} \tag{25}$$

and

$$\tau_{xy,\max} = \frac{V \bullet S_y^{A_z}\left(\frac{b}{2}\right)}{I_y \bullet t_f} \tag{26}$$

Along the web the normal stress function and the shear force one (along the z axis) read

$$\sigma_x(N,M,z) = \frac{N}{A} + \frac{M}{I_y} z \tag{27}$$

and

$$\tau_{xz}(V,z) = \frac{V \bullet S_y^{A_y}(z)}{I_y \bullet t_w} \tag{28}$$

Therefore, the cross-section domain boundary on the first octant of the N,V,M space, $\forall N \in (0;N_b)$, $\forall V \in (0;V_b)$, $\forall M \in (0;M_b)$, is defined imposing that in correspondence to the medium point of the section intrados the resistance condition is:

$$\sqrt{\sigma_x^2 + 3\tau_{xy,\max}^2} = \sigma_b \tag{29}$$

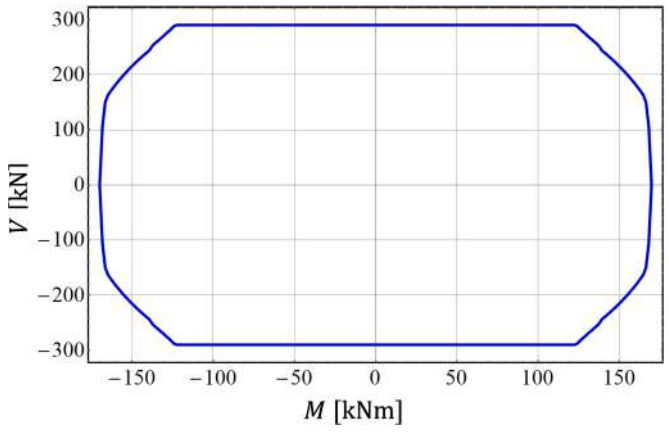

Fig. 6. Reduced elastic domain in M,V plane for IPE360 S235 steel profile.

i.e.

$$\sqrt{\left(\frac{N}{A}+\frac{M}{W_y^E}\right)^2+3\left(\frac{V\bullet S_y^{A_z}\left(\frac{b}{2}\right)}{I_y\bullet t_f}\right)^2}=\sigma_b \tag{30}$$

and finally

$$\left(\frac{N}{A}+\frac{M}{W_y^E}\right)^2+3\left(\frac{V\bullet S_y^{A_z}\left(\frac{b}{2}\right)}{I_y\bullet t_f}\right)^2=\sigma_b^2 \tag{31}$$

and that along the web, $\forall N\in(0;N_b)$, $\forall V\in(0;V_b)$,$\forall M\in(0;M_b)$, $\forall z\in\left(0;\frac{h}{2}-t_f\right)$ the resistance condition is

$$\sqrt{\sigma_x^2+3\tau_{xz}^2}=\sigma_b \tag{32}$$

i.e.

$$\sqrt{\left(\frac{N}{A}+\frac{M}{I_y}z\right)^2+3\left(\frac{V\bullet S_y^{A_y}(z)}{I_y\bullet t_w}\right)^2}=\sigma_b \tag{33}$$

and finally

$$\left(\frac{N}{A}+\frac{M}{I_y}z\right)^2+3\left(\frac{V\bullet S_y^{A_y}(z)}{I_y\bullet t_w}\right)^2=\sigma_b^2 \tag{34}$$

Therefore, for a sufficiently wide number of couples of $\overline{N}$ and $\overline{M}$ values ($0\le\overline{N}\le N_b;0\le\overline{M}\le M_b$), the correspondent limit value of the shear force can be defined as the lower value between

$$V=\left\{\frac{\left[\sigma_b^2-\left(\frac{\overline{N}}{A}+\frac{\overline{M}}{W_y^E}\right)^2\right]I_y^2\bullet t_f^2}{3\left[S_y^{A_z}\left(\frac{b}{2}\right)\right]^2}\right\}^{\frac{1}{2}} \tag{35}$$

and the minimum shear force value obtained by the solution to the following optimization problem

$$\min_{(z)}V \tag{36a}$$

subjected to

$$0\le z\le\frac{h}{2}-t_f \tag{36b}$$

$$\left(\frac{\overline{N}}{A}+\frac{\overline{M}}{I_y}z\right)^2+3\left(\frac{V\bullet S_y^{A_y}(z)}{I_y\bullet t_w}\right)^2\ge\sigma_b^2 \tag{36c}$$

On the other octants of the N,V,M space, the boundary surface can be defined imposing symmetry with respect to the coordinate planes.

The overall domain in the N,V,M space is reported in Fig. 7, referring once again to a IPE360 S235 steel profile.

3. LRPD optimal design procedure

The optimal device to be designed has to fulfill two fundamental goals: 1) the protection of the BWC at the beam ends, ensuring that the acting generalized stresses are within the brittle safe domain previously defined; 2) the realization of suitably selected beam element portions where an appropriate amount of plastic strain energy is dissipated. To reach these goals, the device must exhibit an elastic perfectly plastic behaviour with a suitably prefixed resistance limit. In particular, for given values of axial and shear forces, the device is designed so that it fully plasticizes for a bending moment value which ensures that the three generalized stresses acting at BWC are within the relevant reduced elastic domain. Such a desired effect can be obtained appropriately reducing the cross-section constituting one of the device portions, so producing a resistance reduction. The special device utilized (LRPD), differently to other competitors proposed by other authors in the scientific and technical literature, takes advantage of the particular shape and geometry (stepped cross-sections), and also prevents the undesired elastic flexural stiffness reduction, typical of the other known devices.

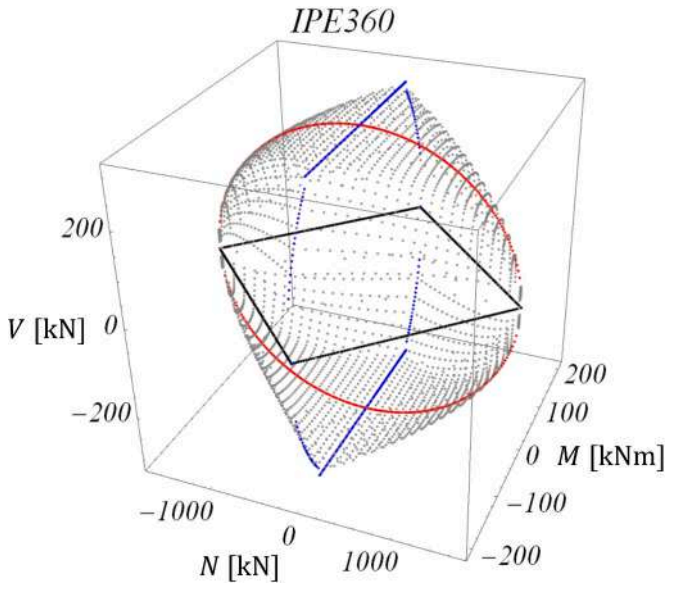

Fig. 7. Reduced elastic domain space for IPE360 S235 steel profile.

Specifically, the LRPD will possess overall dimensions $\ell\times b_p\times h_p$, with ℓ design variable to be determined and $b_p\times h_p$ dimensions of the rectangle circumscribed to the cross-section of the beam element profile to which the device will be connected. It will be utilised to substitute an analogous portion of the I-shaped beam element in correspondence to the beam-columns connection (see Fig. 8 and Table 2) and it must ensure: *i*) a full plasticization of the inner portion for appropriate assigned values of the generalized stresses (N, V, M), preventing dangerous local buckling of the relevant flanges; *ii*) the consistency of the equivalent elastic flexural stiffness, defined as the global flexural stiffness of the portion of length ℓ in the hypothesis of linear elastic behaviour. A complete description of LRPD is reported in [21], while in the appendix a synthetic description of the principal shape, geometrical and mechanical features is reported. In the following, the presence of the welding size will be neglected in the definition of the geometrical and mechanical properties of the relevant cross-sections.

To fulfill the first requirement, the values of N, V and M to be utilized, in correspondence of which the full plasticization of the internal portion of the device is imposed, depend on the response of the structure not equipped by the relevant device. In detail, once the generalized stresses on the BWC to be protected are known, it must be ensured that the device reaches its plastic limit for the couple of the given axial force and a suitable value of the bending moment $M_{\ell im}$; the latter depends on the brittle safe limit behaviour of the outer cross-section of the device realising the welded connection and on the actual distribution of shear force and acting loads. Making reference to Fig. 9, $M_{\ell im}$, the yield bending moment value to be imposed for the inner portion of the device, is given by

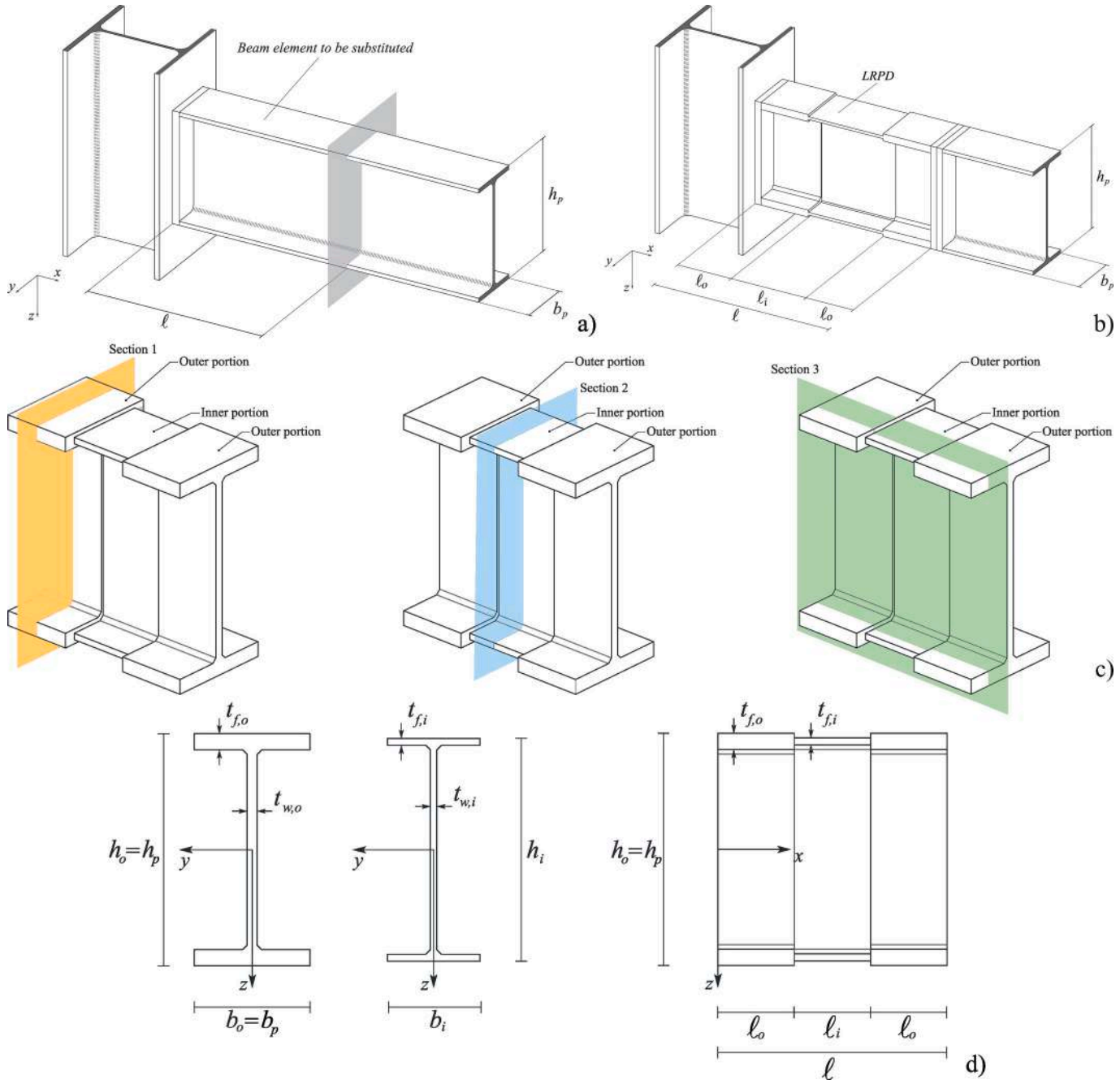

Fig. 8. Sketch of LRPD with main geometric characteristics: a) portion of the original beam to be substituted; b) LRPD inserted at the beam extreme; c) LRPD general 3D view; d) Section 1, Section 2 and Section 3.

$$M_{\ell im} = M_{b,N,V} - V\left(\ell_o + \frac{\ell_i}{2}\right) + \frac{q}{2}\left(\ell_o + \frac{\ell_i}{2}\right)^2 \tag{37}$$

In Eq. (37) $M_{b,N,V}$ is the bending moment value of BWC of the original beam element corresponding to a limit brittle safe condition for the assigned axial force N and shear force V (accordingly with the brittle safe domain defined in the previous section) and q the acting uniformly distributed load along the beam. In the following, the relevant value of the axial force related with $M_{\ell im}$ for the design of the device will be indicated with $N_{\ell im}$. Finally, it is noted that for the evaluation of the limit behaviour of the inner portion of the device (which does not involve any risk of brittle failure) the influence of the shear force will be disregarded.

The device volume is chosen as objective function to be minimized; it is constituted by an inner portion of length ℓ_i and two identical outer portions both of length ℓ_o. Furthermore, with the aim of ensuring the onset of appropriate plastic strain fields within the inner portion, it is necessary to impose a lower bound on ℓ_i, in such a way as to allow a full strain diffusion all across the section depth. Making reference to several studies proposed by the authors (see, e.g. [17], [19], [21], [22]), the most recommended choice is that of defining the minimum length of the inner portion as a function of the original cross-section depth. Namely, $\ell_i = \beta h_p$ is assumed, being h_p the known section depth of the original beam cross-section and β a suitably assigned positive scalar (usually the range $0.5 \leq \beta \leq 1$ is suggested). In particular, it has been verified (see [17]) that the lower bound $\beta = 0.5$ is appropriate for IPE profiles, while $\beta = 1$ is suggested for HE profiles.

Table 2
Geometrical characteristics of the device.

Adopted Symbol	Description
Outer portions	
b_o	Section width
h_o	Section depth
$t_{w,o}$	Web thickness
$t_{f,o}$	Flange thickness
ℓ_o	Length
Inner portion	
b_i	Section width
h_i	Section depth
$t_{w,i}$	Web thickness
$t_{f,i}$	Flange thickness
ℓ_i	Length
Overall device	
ℓ	Total length

3.1. Minimum volume design problem

The design variable vector is

$$\boldsymbol{d}^T = \left| h^* \quad b_i \quad t_{f,i} \quad t_{f,o} \quad \ell_o \right| \tag{38}$$

and the objective function to be minimized (device volume) is

$$\begin{aligned} v(\boldsymbol{d}) &= A_i \ell_i + 2A_o \ell_o \\ &= \left[2b_i t_{f,i} + t_{w,p}\left(h^* - t_{f,i}\right)\right]\ell_i + 2\left[2b_p t_{f,o} + t_{w,p}\left(h^* - t_{f,o}\right)\right]\ell_o = \\ &= \left[2b_i t_{f,i} + t_{w,p}\left(h^* - t_{f,i}\right)\right]\beta h_p + \left[4b_p t_{f,o} + 2t_{w,p}\left(h^* - t_{f,o}\right)\right]\ell_o \end{aligned} \tag{39}$$

where A_i and A_o are the inner and outer cross-section areas, $t_{w,p}$ the web thickness of the original beam cross-section and the equalities $h^* = h_i - t_{f,i} = h_o - t_{f,o}$ have been utilized together with the position $\ell_i = \beta h_p$. In Eq. (39) it is imposed that the web thickness of the inner and of the outer portion are equal to each other and equal to that of the web of the original beam cross-section.

The minimum volume design problem can be written in the following form:

$$\min_{(\boldsymbol{d})} v(\boldsymbol{d}) \tag{40a}$$

subjected to

$$\boldsymbol{d}_{\ell ow} \le \boldsymbol{d} \le \boldsymbol{d}_{upp} \tag{40b}$$

$$\boldsymbol{A}_{eq}\boldsymbol{d} = a_{eq} \tag{40c}$$

$$\boldsymbol{A}_{in}\boldsymbol{d} \le a_{in} \tag{40d}$$

$$G_{eq}(\boldsymbol{d}) = g_{eq} \tag{40e}$$

$$G_{in}(\boldsymbol{d}) \le g_{in} \tag{40 f}$$

In the above reported problem, the adopted scalar functions, vectors and matrices have the following form:

$$\boldsymbol{d}_{\ell ow}^T = |\,0 \quad 3t_{w,p} \quad 0 \quad t_{f,p} \quad 0\,| \tag{41}$$

$$\boldsymbol{d}_{upp}^T = \left| h_p - t_{f,p} \quad b_p \quad t_{f,p} \quad \frac{h_p}{2} \quad \infty \right| \tag{42}$$

$$\boldsymbol{A}_{eq} = |\,1 \quad 0 \quad 0 \quad 1 \quad 0\,|;\ a_{eq} = h_p \tag{43}$$

$$\boldsymbol{A}_{in} = \left| 0 \quad 1 \quad -18\sqrt{\frac{235}{\sigma_0}} \quad 0 \quad 0 \right|,\ a_{in} = 3t_{w,p} \tag{44}$$

$$\begin{aligned} G_{eq}(\boldsymbol{d}) = {} & b_i\, t_{f,i} h^* \sigma_0 + t_{w,p}\sigma_0 \left(\frac{h^* - t_{f,i}}{2}\right)^2 - M_{b,N,V} + V\left(\ell_o + \frac{\ell_i}{2}\right) \\ & - \frac{q}{2}\left(\ell_o + \frac{\ell_i}{2}\right)^2 \end{aligned} \tag{45}$$

with

$$g_{eq} = \frac{N_{\ell im}^2}{4t_{w,p}\,\sigma_0} \tag{46}$$

if the neutral axis cuts through the cross-section web, or

$$G_{eq}(\boldsymbol{d}) = \frac{N_{\ell im}}{2}\left[2t_{f,i} + \frac{t_{w,p}}{b_i}\left(h^* - t_{f,i}\right) - \frac{N_{\ell im}}{2b_i f_y} - \left(h^* + t_{f,i}\right)\right]$$

$$+ \sigma_0\left[b_i t_{f,i} + \frac{t_{w,p}}{2}\left(h^* - t_{f,i}\right)\right]\left[\left(h^* + t_{f,i}\right) - t_{f,i} - \frac{t_{w,p}\left(h^* - t_{f,i}\right)}{2b_i}\right] - M_{b,N,V} + V\left(\ell_o + \frac{\ell_i}{2}\right) - \frac{q}{2}\left(\ell_o + \frac{\ell_i}{2}\right)^2 \tag{47}$$

with

$$g_{eq} = 0 \tag{48}$$

if the neutral axis cuts through one of the cross-section flanges,

$$G_{in}(\boldsymbol{d}) = \frac{\beta h_p}{\ell_o} - \frac{4b_i t_{f,i}^3 + 12b_i t_{f,i} h^{*2} + 2t_{w,p}\left(h^* - t_{f,i}\right)^3}{2b_p t_{f,o}^3 + 6b_p t_{f,o} h^{*2} + t_{w,p}\left(h^* - t_{f,o}\right)^3}$$

$$\left(\frac{2b_p t_{f,o}^3 + 6b_p t_{f,o} h^{*2} + t_{w,p}\left(h^* - t_{f,o}\right)^3 - 12I_p}{12I_p - 2b_i t_{f,i}^3 - 6b_i t_{f,i} h^{*2} - t_{w,p}\left(h^* - t_{f,i}\right)^3}\right) \tag{49}$$

with

$$g_{in} = 0 \tag{50}$$

Eqs. (41) and (42) define lower and upper bounds for the design variables, respectively, where $t_{f,p}$ is the thickness of the original cross-section flanges.

Eq. (43) define an equality linear technological constraint related to the internal lever arm, respecting the position $h_o = h_p$.

Eq. (44) define an inequality linear constraint ensuring the belonging of the cross-section of the inner portion to the Class 1 [22] of ductility, preventing dangerous buckling effects.

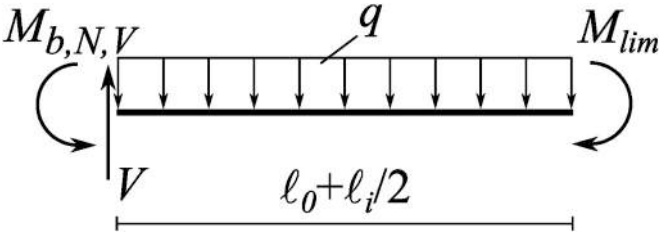

Fig. 9. Definition of $M_{\ell im}$.

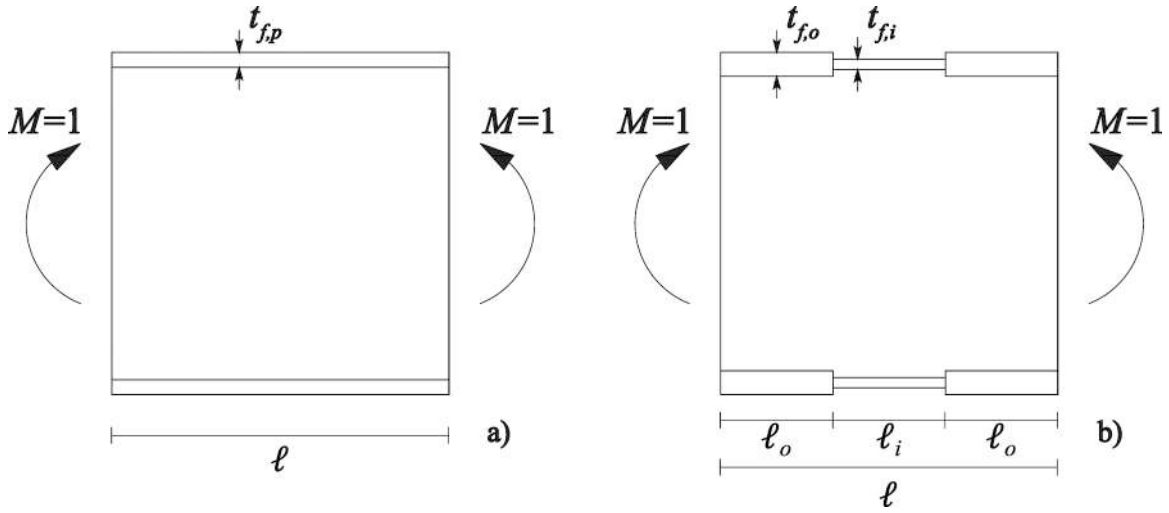

Fig. 10. Evaluation of the equivalent bending stiffness: (a) given beam element portion; (b) LRPD.

Eqs. (45)-(48) define equality non-linear constraints ensuring the plasticization of the inner portion cross-section for the assigned couple of values $N_{\ell im}, M_{\ell im}$ imposing the relevant cross-section entirely plasticized (see, e.g. [21] and the Appendix).

Eqs. (49) and (50) define an inequality non-linear constraint ensuring the consistency of the equivalent elastic flexural stiffness.

These last equations can be deduced by imposing (see Fig. 10) that the relative rotation $(\Delta\varphi_{LRPD})$ between the bound sections of the device subjected to the bending moment $M = 1$, evaluated as follows:

$$\Delta\varphi_{LRPD} = 2\int_0^{\ell_o} \frac{1}{EI_o}dx + \int_0^{\ell_i} \frac{1}{EI_i}dx \tag{51}$$

equals the one $(\Delta\varphi_p)$ between the end sections of the substituted original beam portion subjected to the same bending moment given as:

$$\Delta\varphi_p = \int_0^{\ell} \frac{1}{EI_p}dx \tag{52}$$

where I_p is the moment of inertia of the beam section connected to the device and E is the Young's modulus of the material. As already stated in many papers (see, e.g. [17], [19], [21], [22]), the previous relations lead to the following equality:

$$\frac{\ell_i}{\ell_o} = 2\frac{I_i}{I_o}\left(\frac{I_o - I_p}{I_p - I_i}\right) \tag{53}$$

being the function on the right-hand side an increasing one with respect to I_o. From Eq. (53), with appropriate mathematics, the position (49)-(50) can be obtained, written as function of the design variables.

The above formulated problem is a non-linear programming one and for its solution a suitable solver can be utilized by adopting an interior-point algorithm.

4. Application

In order to validate the efficacy of the use of LRPD and to test the solidity of the proposed design approach, the frame sketched in Fig. 11a is examined. In the case under examination $L_1 = 6.00\,m$, $L_2 = 4.00\,m$, $H_1 = 5.00\,m$, $H_2 = 4.00\,m$, the adopted material is a S235 steel grade ($E = 210\,GPa$, $\sigma_0 = 235\,MPa$) with an elastic perfectly plastic behaviour.

The design of the structural cross-sections has been performed following the requirements of the Italian building code [5] for both ultimate limit state (static and seismic load conditions) and serviceability limit state (static and seismic load conditions). The assumed input data are: usage class III, soil category B, topographic category T1 and nominal life equal to 100 years. The prescribed distributed load (B2 category) are: permanent structural load $G_1 = 2.5\,kN/m^2$ for both the floors, permanent non-structural load $G_2^I = 4.0\,kN/m^2$ for the first floor and $G_2^{II} = 2.5\,kN/m^2$ for the second floor, variable load $Q = 3.0\,kN/m^2$ for both the floors. In Fig. 11b the frame and its basic vertical loads are reported taking into account that the slab influence depth is equal to 5 m for the first span (beams 7 and 9) and to 3 m for the second span (beams 8 and 10).

The cross-sections obtained by solving the previously cited classical standard code design are reported in Fig. 12.

As is well known, the effected design takes into account (through specific structure factors suggested by the standards) the capacity of the steel structure to behave beyond its elastic limit and to produce plastic deformations dissipating appropriate amount of plastic strain energy. For frame structures, the relevant plastic deformations are substantially represented by plastic curvatures located at the end of the beams, namely in correspondence to the BWC of the beam-column connections. Taking into account the risk of brittle behaviour of the BWC, it is necessary to avoid this occurrence making sure that they always behave in a purely elastic manner.

To check the real elastic plastic response of the structure and in particular of the welded connections between beams and columns, it is necessary to perform a step by step elastic plastic dynamic analysis, as is also planned by the building code [5], adopting as input the ground acceleration suitably obtained by the relevant response spectrum, considering the seismic characteristics of the site where the building is located. For the case under examination the selected site is Palermo (Sicily, Italy) and the number of the considered accelerograms is seven. The analysis has been performed by means of SeismoStruct2023 software adopting infrmFB as element class and stl_bl as material mechanical model assuming an elastic perfectly plastic behaviour.

The time histories of the mean bending moment response for both ends of each beam are reported in Fig. 13. As expected, the obtained results show that in beams 7 and 8 the limit elastic bending moment is exceeded and, as a consequence, an appropriate ductile behaviour must be ensured. The results for beams 9 and 10 indicate that the bending moment is always below the elastic limit although the maximum values are very close to the relevant elastic limit ones.

In Fig. 14 the bending moment vs bending curvature diagrams related to beams 7 and 8 are reported, respectively, together with the bending moment elastic domain.

By the results reported in Fig. 14 it is possible to remark that both the beams behave slightly above their elastic limit so that their ductility

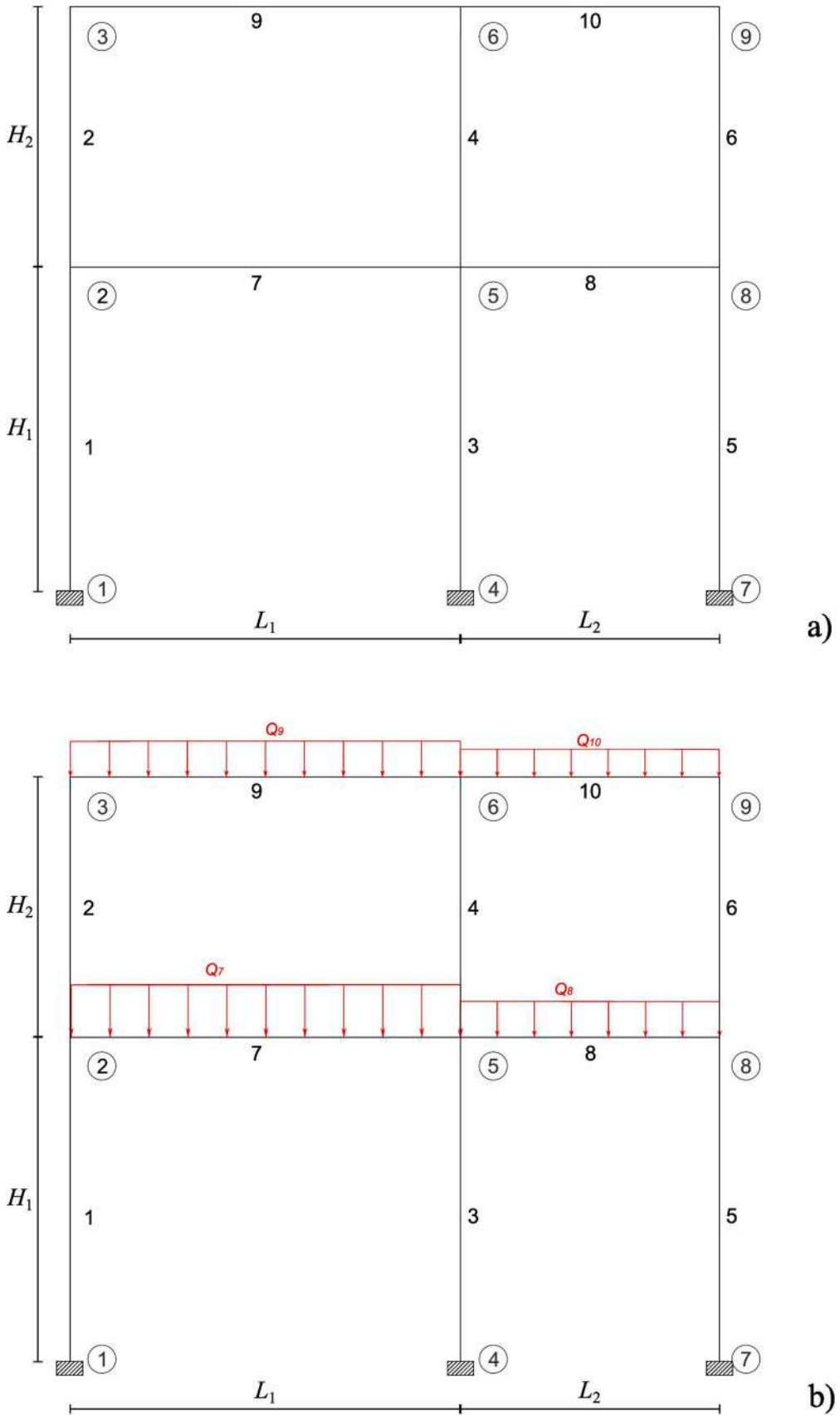

Fig. 11. Plane frame: a) geometry and identification of beam elements and nodes; b) acting vertical loads.

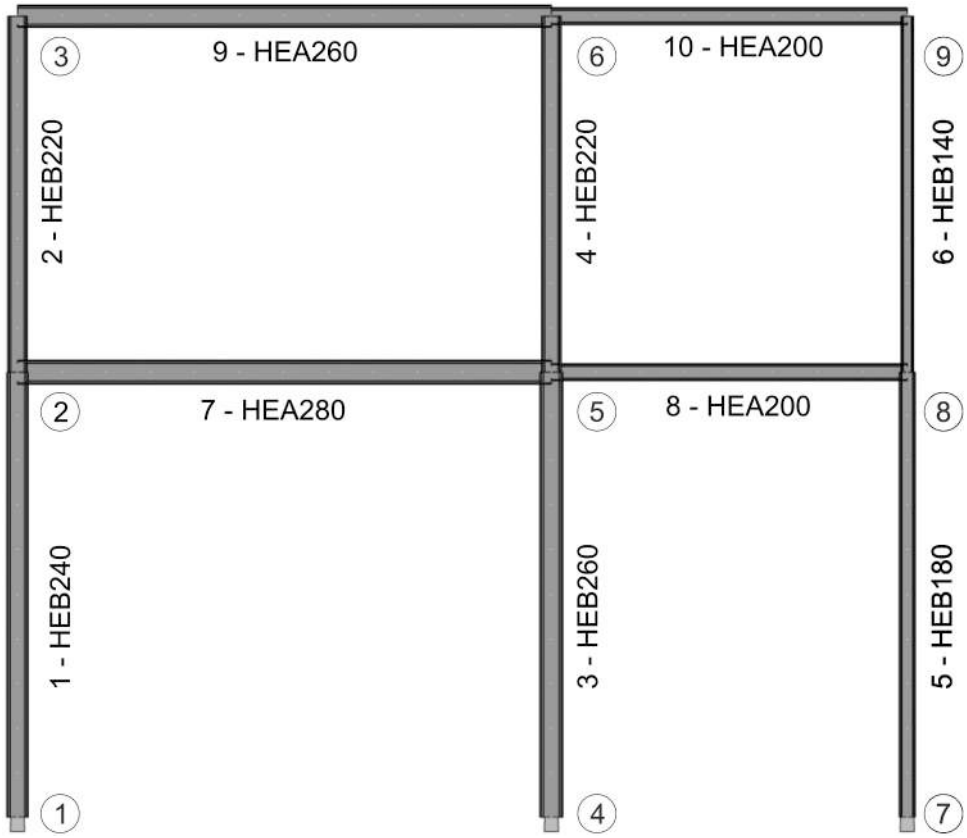

Fig. 12. Plane frame: beam element cross-section design.

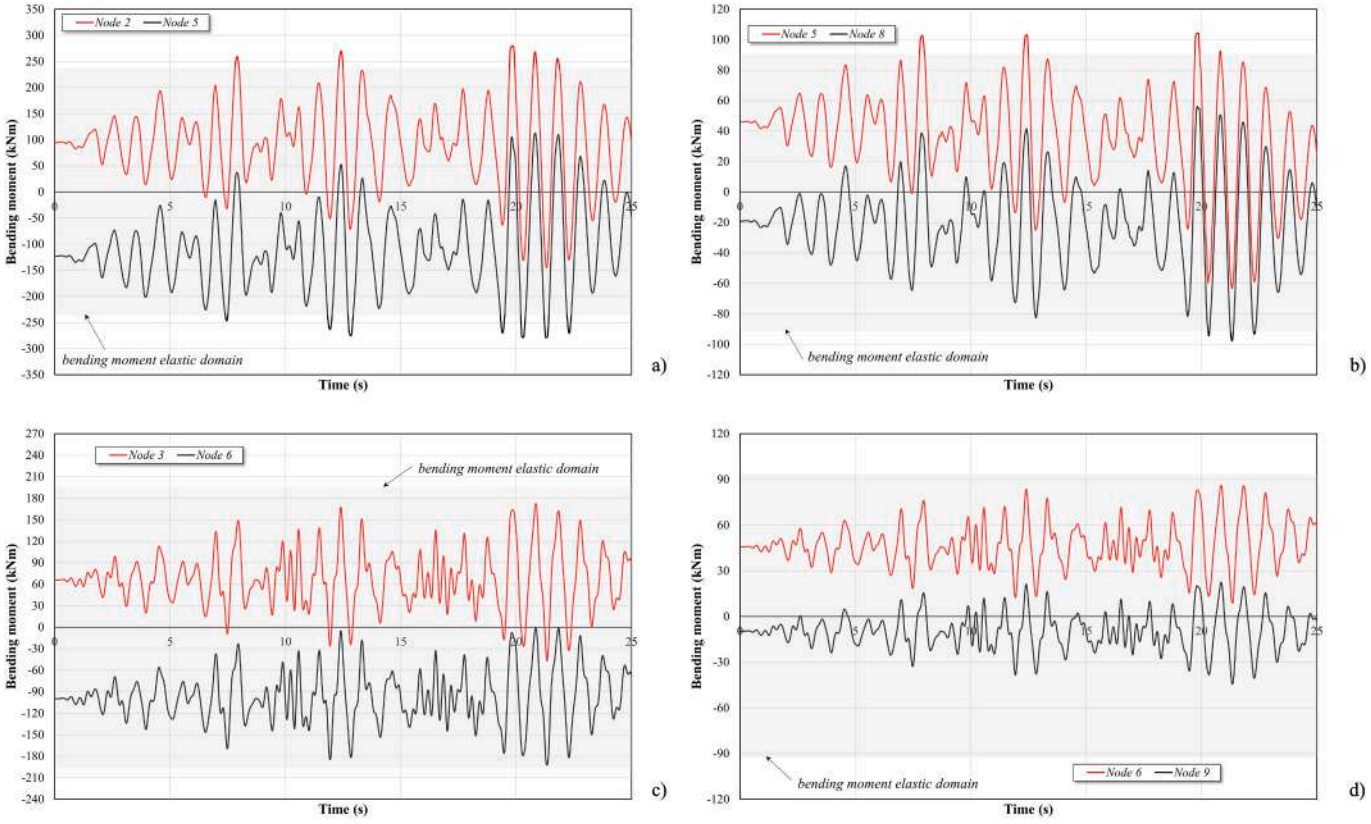

Fig. 13. Mean bending moment response vs time: a) beam 7; b) beam 8; c) beam 9; d) beam 10.

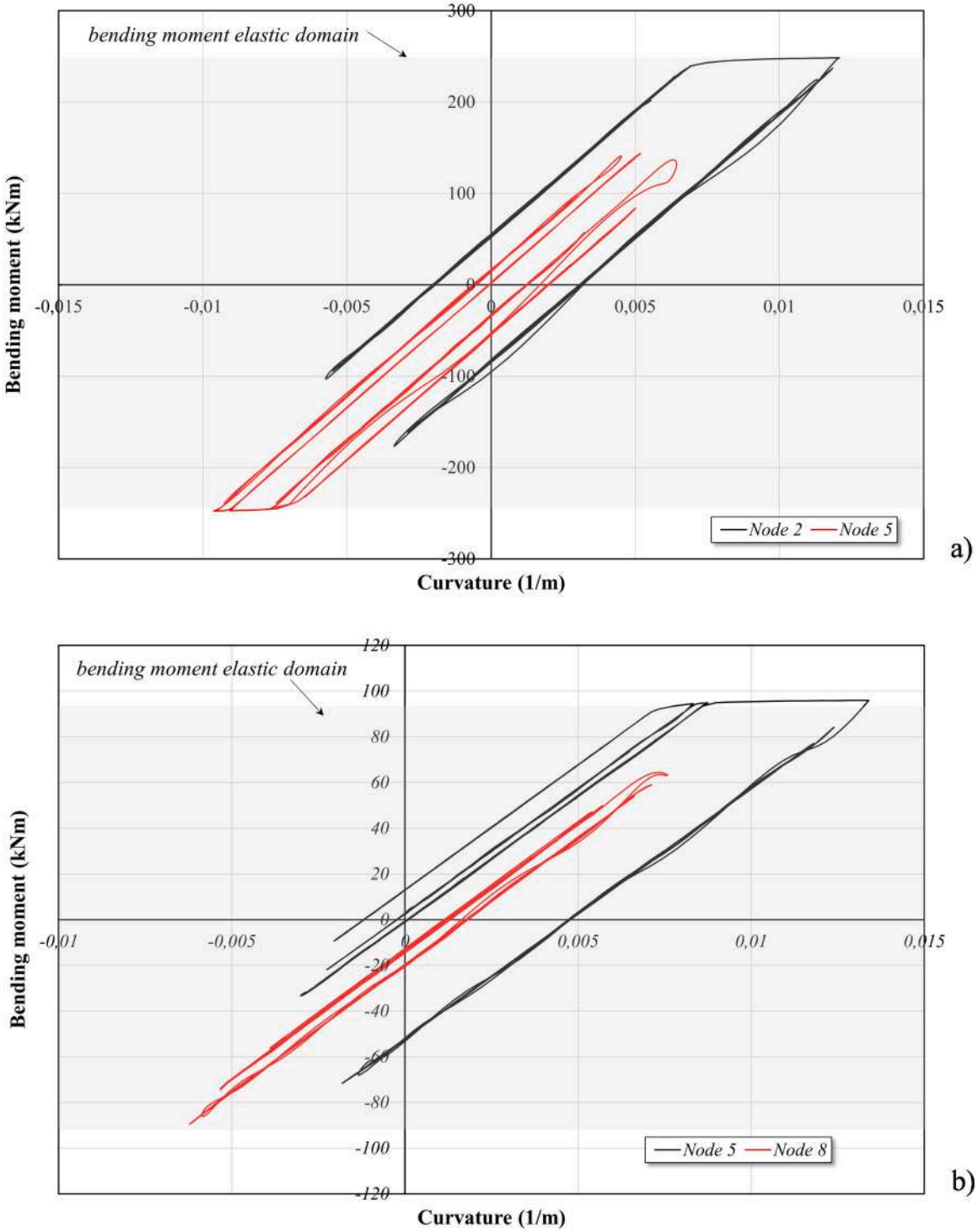

Fig. 14. Bending moment vs curvature: a) beam 7; b) beam 8.

Table 3
Limit bending moment values.

Beam	$M_{e\curvearrowleft}$ [kN/m]	$M_{p\curvearrowleft}$ [kN/m]	M_{br} [kN/m]
7	238.06	261.32	185.63
8	91.32	100.93	71.22
9	196.55	216.15	152.95
10	91.32	100.93	71.12

features are not satisfactorily used. Further, the bending moment reported in Fig. 13 are those arising in the beam section connected to the column, i.e. the BWC, where the risk of a brittle rupture is very high. Following the actual standards (see Table 4.2. XIV of [5]) the generalized stresses (N, V, M) acting in a such a section should not exceed the boundary of the brittle safe domain already defined in Section 2. In Table 3, the mean of the limit brittle bending moment M_{br}, is reported for the beams, together with the relevant values of the limit elastic bending moment $M_{e\curvearrowleft}$ and of the yield bending moment $M_{p\curvearrowleft}$.

For a better understanding of the risk of a brittle failure in Fig. 15 the

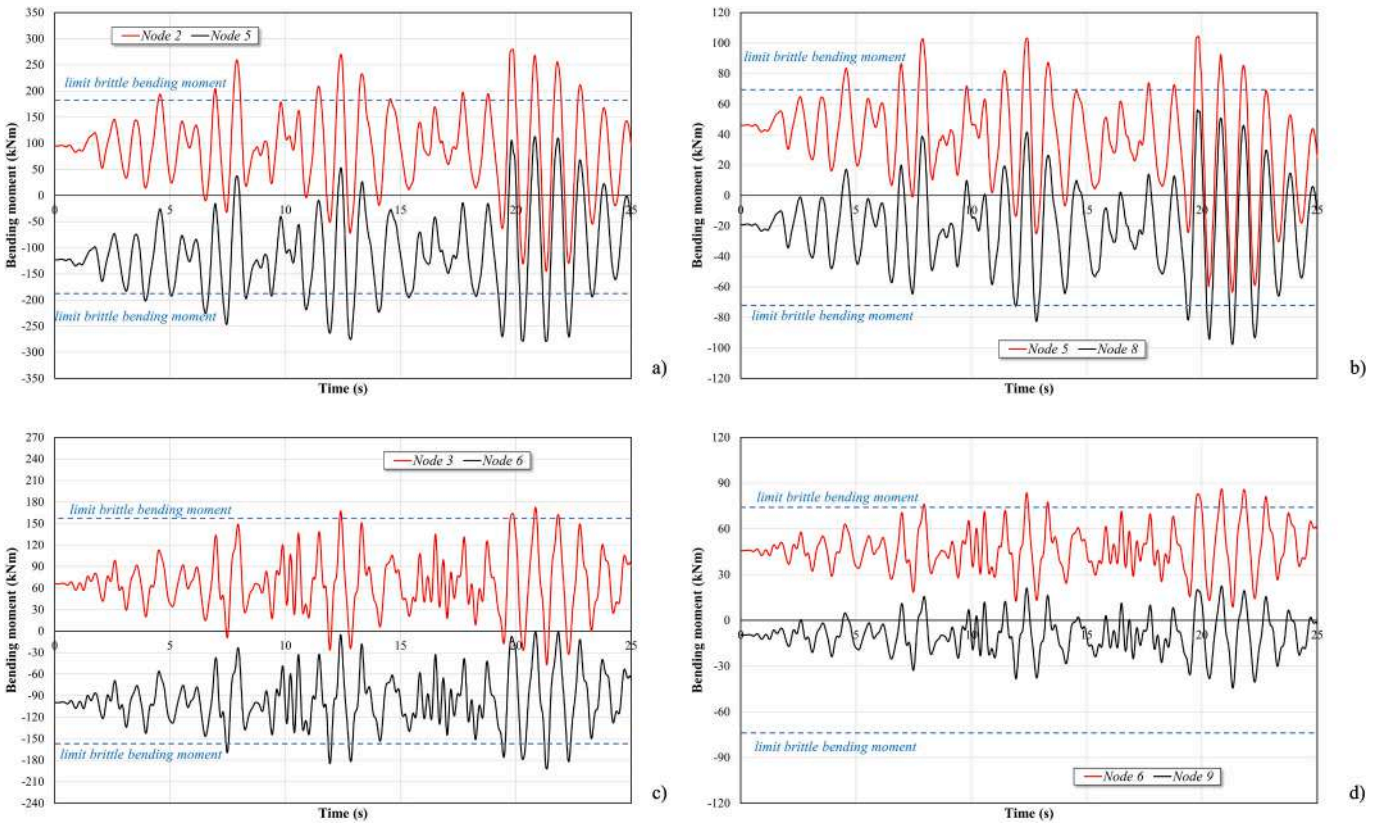

Fig. 15. Mean bending moment response vs time (dashed lines indicate limit brittle bending moment): a) beam 7; b) beam 8; c) beam 9; d) beam 10.

Table 4
Geometric characteristics of LRPDs in mm.

Beam	ℓ_o	b_o	h_o	$t_{f,o}$	ℓ_i	b_i	h_i	$t_{f,i}$
7	173	280	270	20	270	231	263	13
8	47	200	190	20	190	199	180	10
9	81	260	250	23	250	123	232	13
10	233	200	200	22	190	113	170	10

same time histories already in Fig. 13 are reported once again with the indication of the limit brittle bending moment just defined.

An examination of Fig. 15 clearly demonstrates that the bending moment acting at the ends of all the beams often exceeds the corresponding value of the limit brittle bending moment indicating that the risk of a brittle rupture is high.

It follows that it is absolutely necessary to protect the welded connections of all the beams. In order to reach this goal, i.e. to ensure the safe brittle behaviour of the BWC and with the aim of inciting a wider ductile behaviour of the structure, the proposed design approach must be implemented. The optimal LRPD are designed by solving problem (40), where for each device $N_{\ell im}$ is taken as the maximum value of the relevant time history response.

The geometric characteristics of the obtained LRPDs are reported in Table 4. The optimal design problem has been solved by the "fmincon" solver, present in the Matlab Optimization toolbox, that utilizes an interior-point algorithm for the numerical solution of non-linear minimization problems.

The LRPDs, so designed, have been placed at both beam ends and, consequently, a new step by step elastic plastic dynamic analysis has been performed, adopting -as input- the same load conditions.

In Fig. 16 the time histories of the mean bending moment response at the ends of beams 7, 8, 9 and 10 equipped with LRPDs are reported. Furthermore, in the same figures, the limit brittle bending moment corresponding to the section of the outer portion of the related LRPD is also sketched. From an examination of these figures, it is easy to recognize the efficacy of the proposed design approach aimed to preserve the relevant cross-sections by the dangerous brittle failure.

To verify the good behaviour of LRPDs as plastic activators in Fig. 17 the time histories of the mean bending moment response at LRPD midsection for beams 7, 8, 9 and 10 are reported, while in Fig. 18 the mean bending moment response vs bending curvature for each LRPD is reported grouped for each beam. These last results clearly show the good ability of the structure equipped with the relevant devices to dissipate an appropriate amount of plastic energy.

To check the capability of the structure equipped with the relevant devices to provide an acceptable post elastic behaviour, the response in terms of drifts and rotations has been computed. In Fig. 19 the obtained results in terms of drifts are compared with the analogous results related to the original frame structure and in Fig. 20 the analogous comparison is reported in terms of rotations.

The latter comparisons show once more the efficacy of the structure equipped with the proposed device. In particular, the maximum drifts of the structure equipped with the devices are not greater than the ones related with the original structure as well as the maximum rotations of the nodes of the structure equipped with the devices are not greater than the ones related with the original structure, with the exception of node 9 (see Fig. 20 f) where the maximum rotation in presence of the devices is in any case very small and therefore compatible with a viability of the structure.

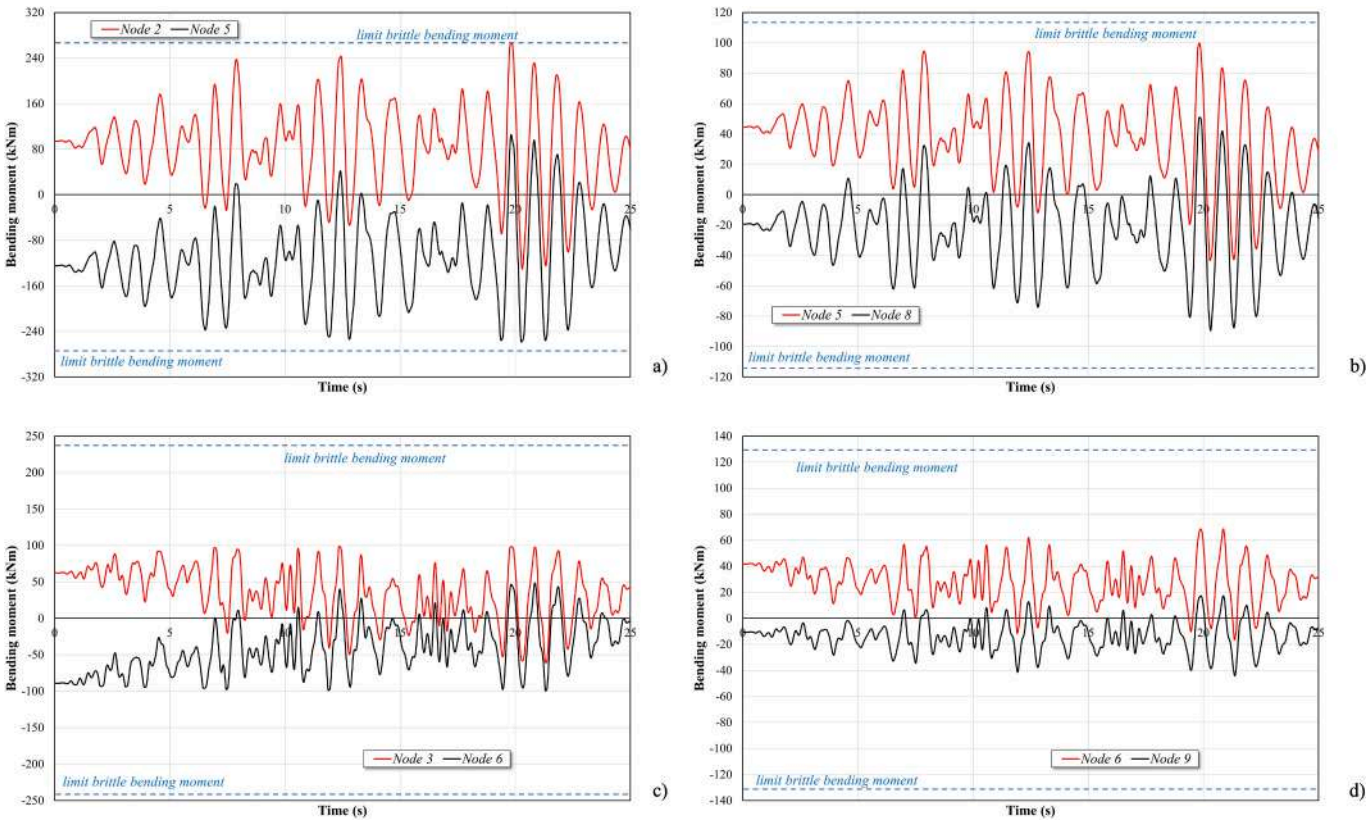

Fig. 16. Mean bending moment response vs time for frame equipped with LRPD: a) beam 7; b) beam 8; c) beam 9); d) beam 10).

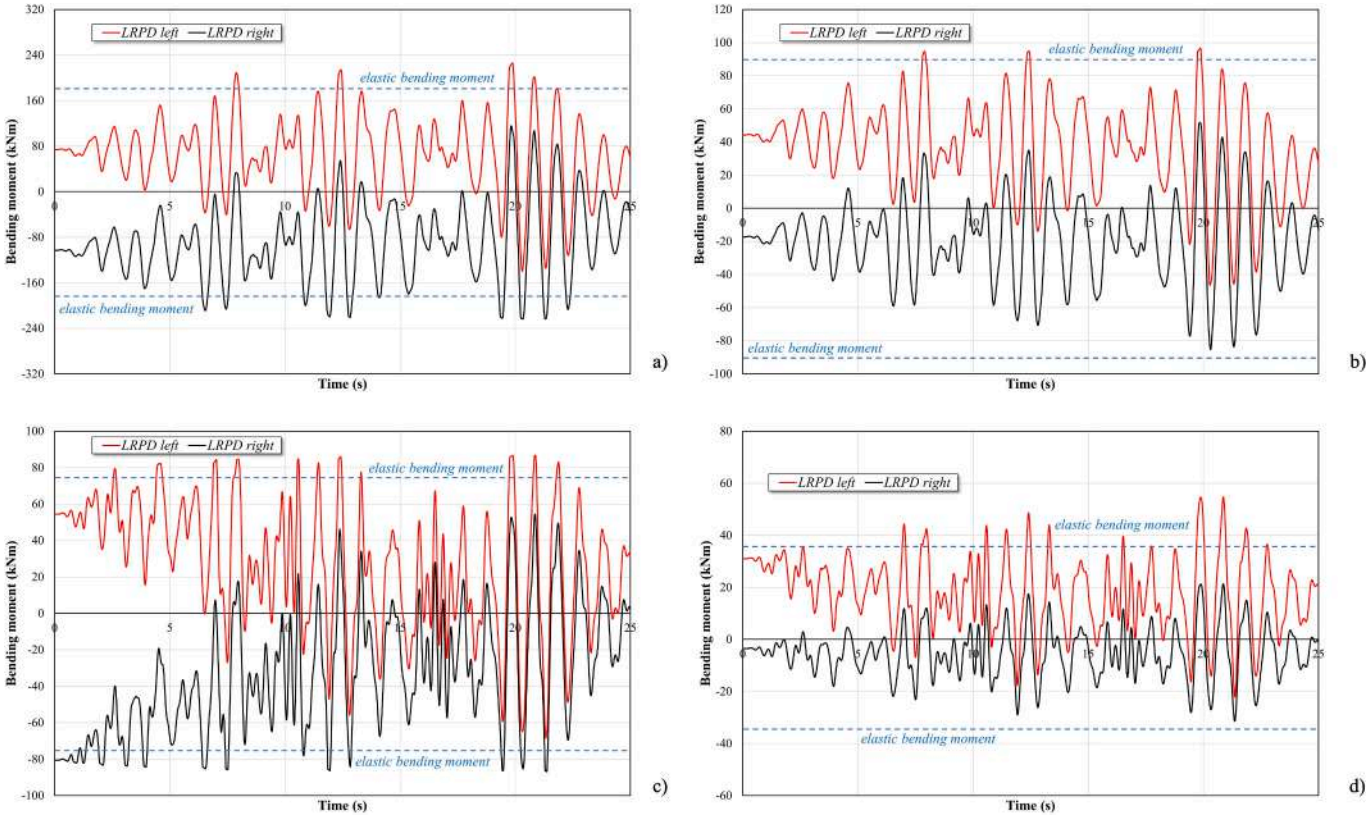

Fig. 17. Mean bending moment response vs time for frame equipped with LRPD: a) beam 7; b) beam 8; c) beam 9); d) beam 10).

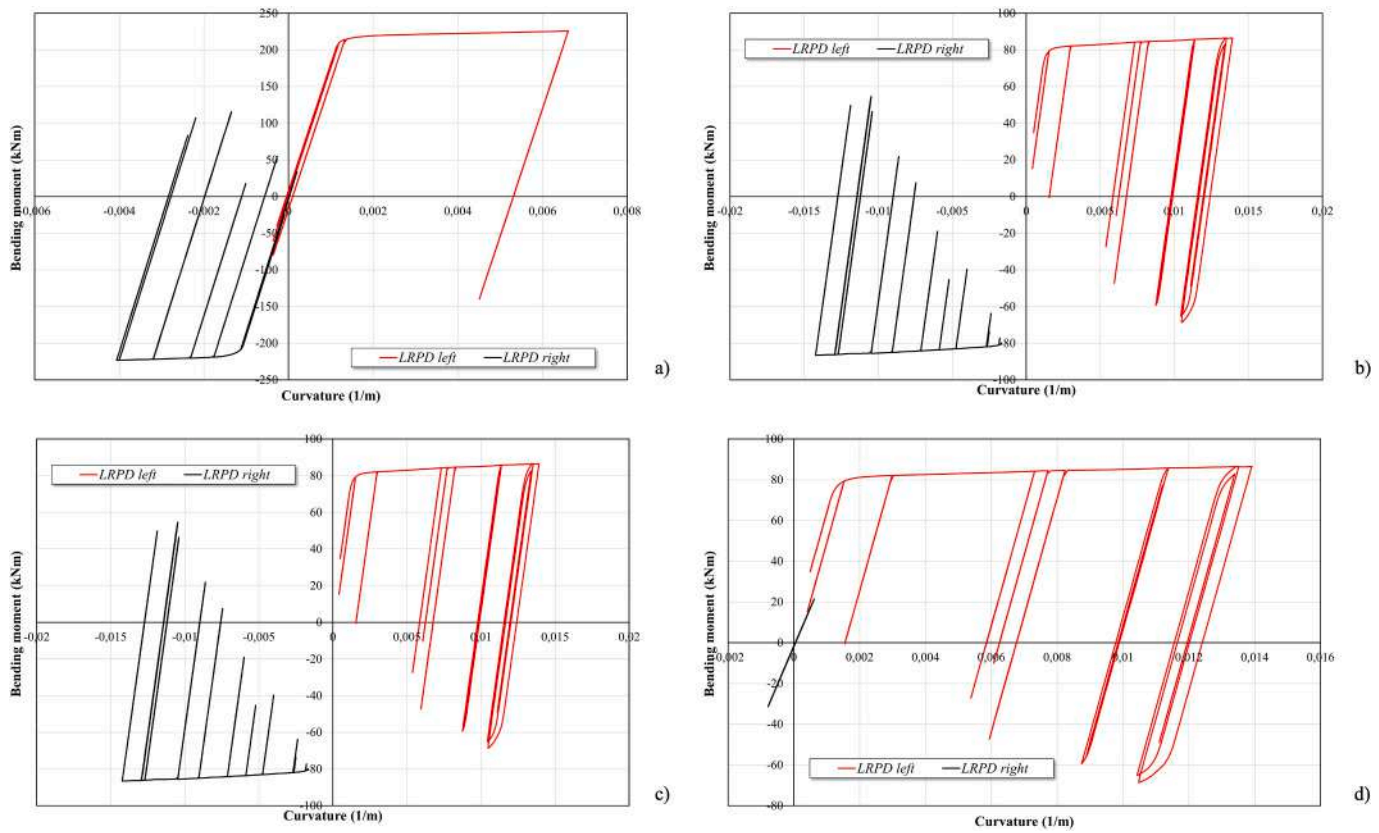

Fig. 18. Bending moment vs curvature: a) beam 7; b) beam 8; c) beam 9; d) beam 10.

In order to make a complete judgement on the use of LRPDs, it was considered useful to compare the effect of using these devices with other devices known in scientific literature and recognised by international standards. In particular, reference is made to the dogbones, belonging to the wider class of RBS connections.

Referring to FEMA 350 [28], the size of the dogbone is reported in Fig. 21 and specified in Table 5. Once again, a dynamic elastic-plastic analysis was performed for the frame equipped with the dogbones, always utilizing the same accelerograms considered for the original structure.

In Fig. 22 the time histories of the mean bending moment response at the ends of beams 7, 8, 9 and 10 equipped with the dogbones are reported. Furthermore, in the same figures, the limit brittle bending moment corresponding to the same sections are also sketched. From an examination of these figures, it is easy to recognize that the dogbone does not ensure the complete protection of the relevant cross-sections by the dangerous brittle failure.

Furthermore, to evaluate the behaviour of dogbones as plastic activators in Fig. 23 the time histories of the mean bending moment response at dogbone midsection for beams 7, 8, 9 and 10 are reported, while in Fig. 24 the mean bending moment response vs bending curvature for each dogbone is reported grouped for each beam. These last results show that even the dogbone intervention provides a structure capable of dissipating an appropriate amount of plastic energy.

Finally, to complete the desired comparison, the response in terms of drifts and rotations for the structure equipped with the dogbones has been computed. In Fig. 25 the obtained results in terms of drifts are compared with the analogous results related to the original frame structure and in Fig. 26 the analogous comparison is reported in terms of rotations, also proving the effectiveness of the application of dogbones.

As a last comparison, the midspan vertical deflection of the beams has been calculated for the original structure, for the structure equipped with the LRPD and for the structure where the dogbones are used. The obtained results for load serviceability conditions are summarized in Table 6 and they show that, as expected, just the LRPD solution ensures the consistency of the elastic flexural stiffness of the involved beams.

Ultimately, therefore, it can be stated that both devices (LRPDs and dogbones) result in an overall improvement of the behaviour of the structure, but only LRPDs fulfill all the desired requirements relating to the prevention of brittle failure risk and a high degree of ductile behaviour causing the minimum disturbance to the behaviour of the original structure behaviour.

5. Conclusions

This paper has been devoted to the proposal of a special design procedure for steel frames characterized by the presence of moment resisting connections, represented by rigid and full-strength connections between columns and beams realized by means of welded and bolted steel plates. The new proposed design strategy ensures: a) the achievement of structures safe with respect to any risk of brittle failure, related to the dangerous possible transition from ductile to brittle behaviour of the beams' end section realising the welded connection; b) the achievement of structures capable of exhibiting resistance capacities beyond their elastic limit and of dissipating an appropriate amount of plastic strain energy. One of the main novelties of the present study relates to in the introduction of suitable brittle safe domains for I-shaped cross-sections, described in a suitable analytic form and represented in the N, V, M space. The definition of these domains is essential for the development of the computational procedure. The latter is performed in

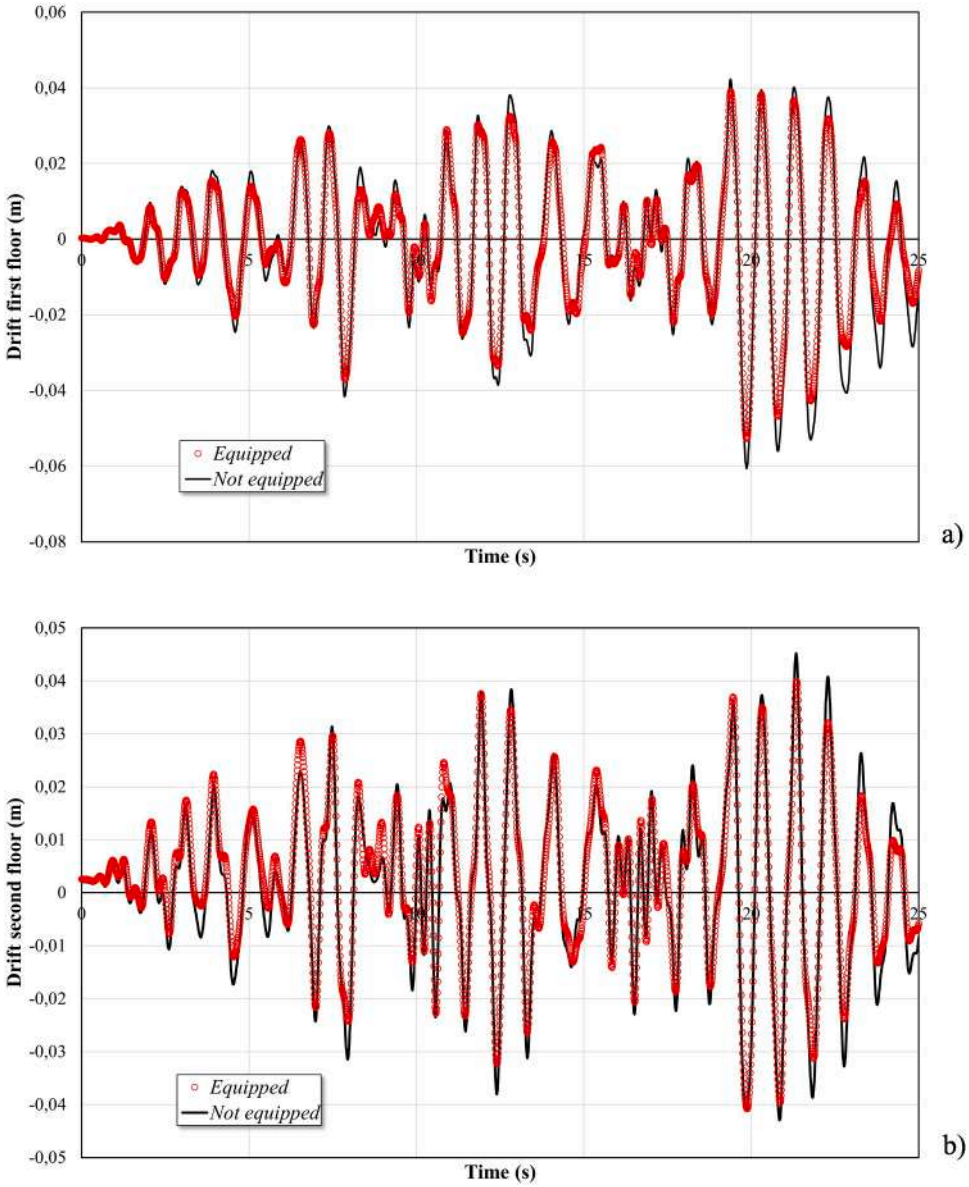

Fig. 19. Drift vs time: a) first floor; b) second floor.

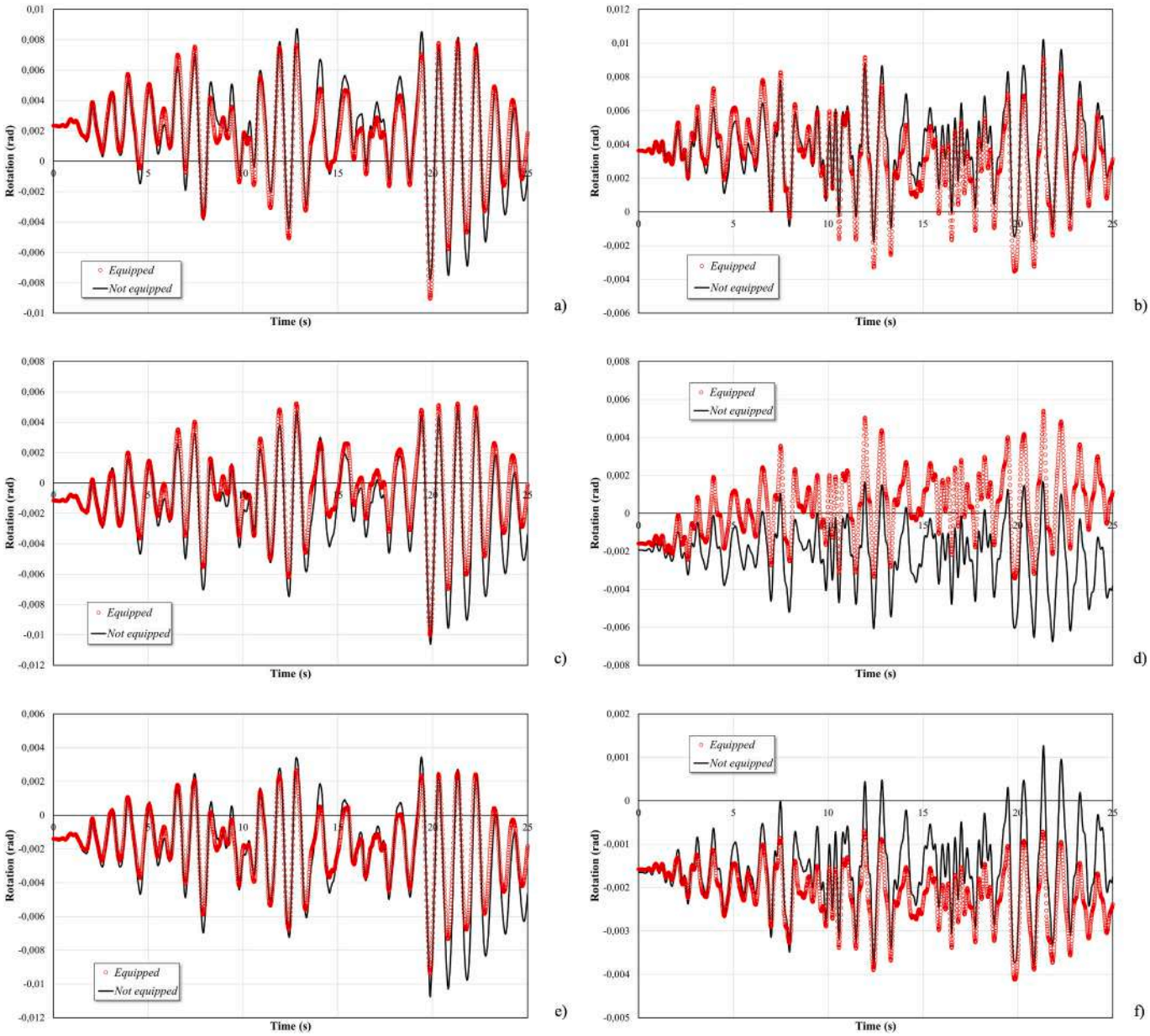

Fig. 20. Rotation vs time: a) Node 2; b) Node 3; c) Node 5; d) Node 6; e) Node 8; f) Node 9.

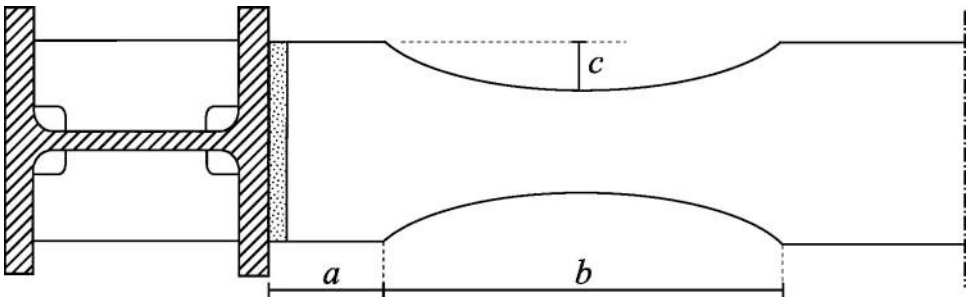

Fig. 21. Geometric characteristic of dogbone (from FEMA 350).

Table 5
Geometric characteristics of dogbones in mm.

Beam	*a*	*b*	*c*
7	140	210	56
8	100	150	40
9	130	195	52
10	100	150	40

four subsequent steps: i) a classical standard code design is obtained by a standard modal analysis referring to the relevant response spectrum; ii) the real behaviour of the structure so designed is checked by performing a step by step elastic plastic dynamic analysis to identify the beam ends where the elastic plastic behaviour is required; iii) the limit value of the relevant bending moment to impose at the selected cross-sections for ensuring a safe brittle behaviour is determined on the ground of the cited brittle safe domain; iv) the optimal LRPDs to be placed at the ends of the beams, which ensure the fulfilling of the previously defined safe condition, are obtained by solving suitably formulated optimal design problems. In the application stage, a two spans two floors plane steel frame has been considered. The obtained results confirmed that the standard code design is exposed to the risk of brittle failure, and it exhibits a very limited ductile behaviour; on the contrary, the frame equipped with the LRPD and designed by means of the proposed procedure possesses both the desired requisites: it is safe against any brittle damage and it is able to dissipate an appropriate amount of plastic strain energy. The reliability of the proposed procedure as well as the effectiveness of the utilized devices has been confirmed by the comparison made with the dogbone devices. Indeed, the results clearly showed that the classical RBS devices result in a reduced protection of BWC but they do not provide any protection against undesired brittle failure. The proposed computational procedure is sufficiently quick and simple; it employes the analytical form of the safe brittle domains here defined, some suitable standard technical software and the "fmincon" solver, present in the Matlab Optimization toolbox, that utilizes an interior-point algorithm for the numerical solution of non-linear minimization problems.

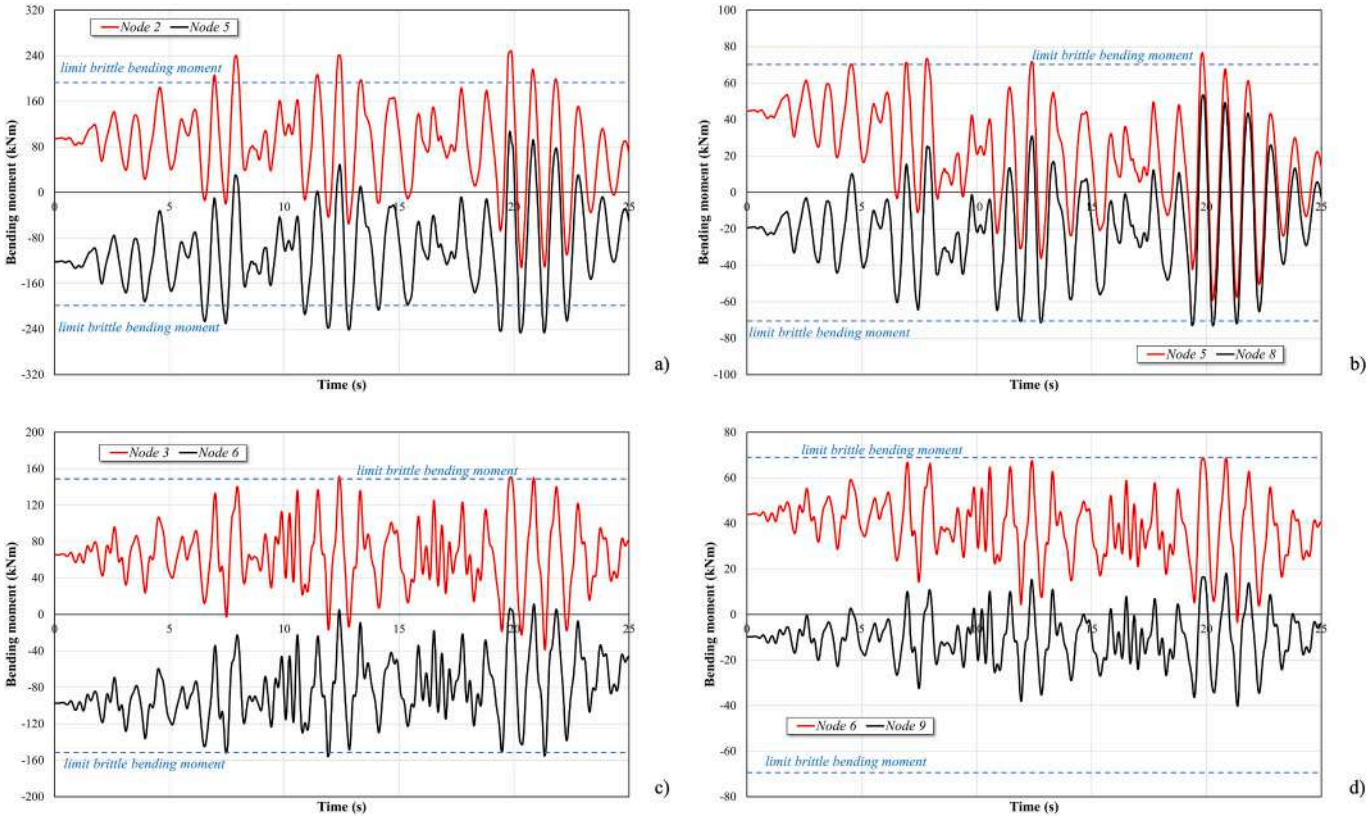

Fig. 22. Mean bending moment response vs time for frame equipped with dogbone: a) beam 7; b) beam 8; c) beam 9); d) beam 10).

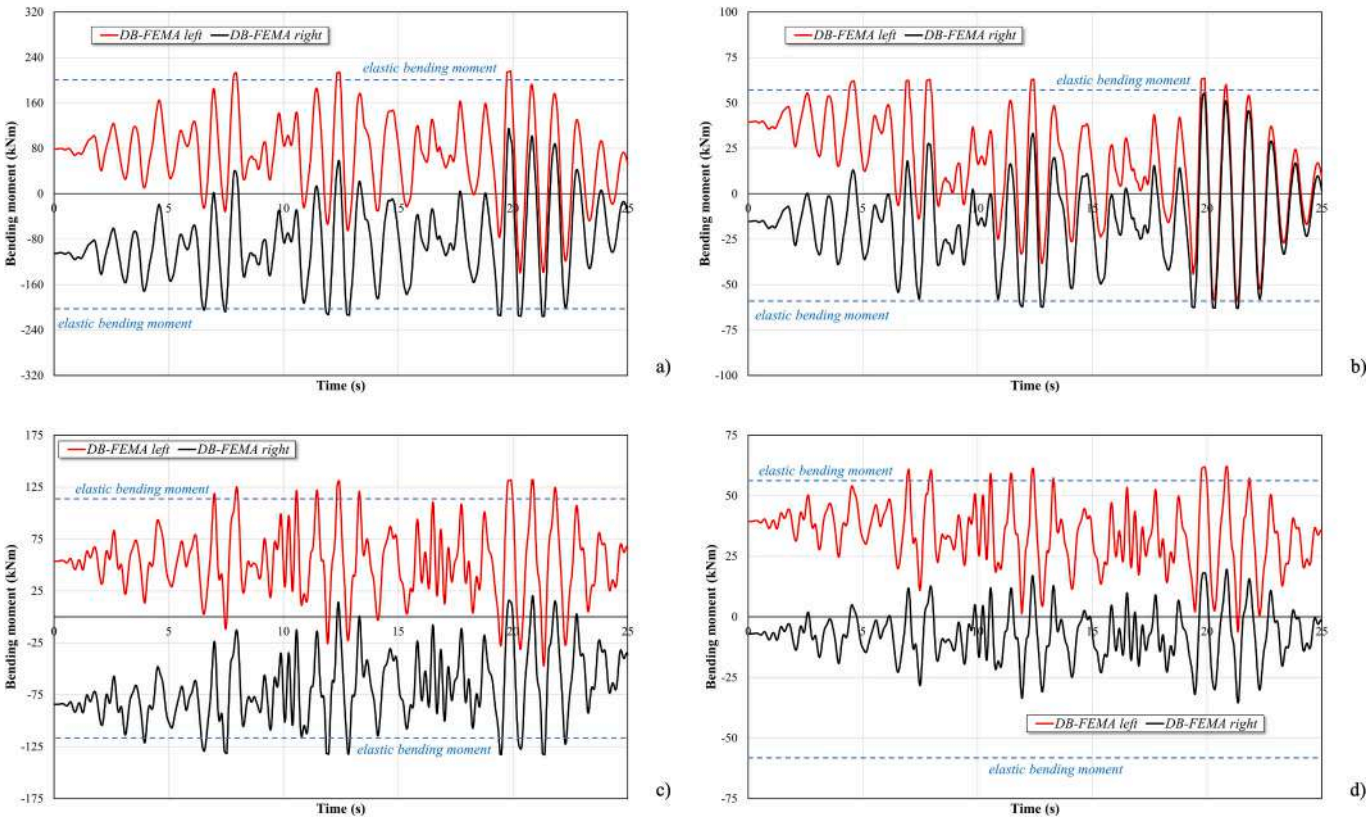

Fig. 23. Mean bending moment response vs time for frame equipped with dogbones: a) beam 7; b) beam 8; c) beam 9); d) beam 10).

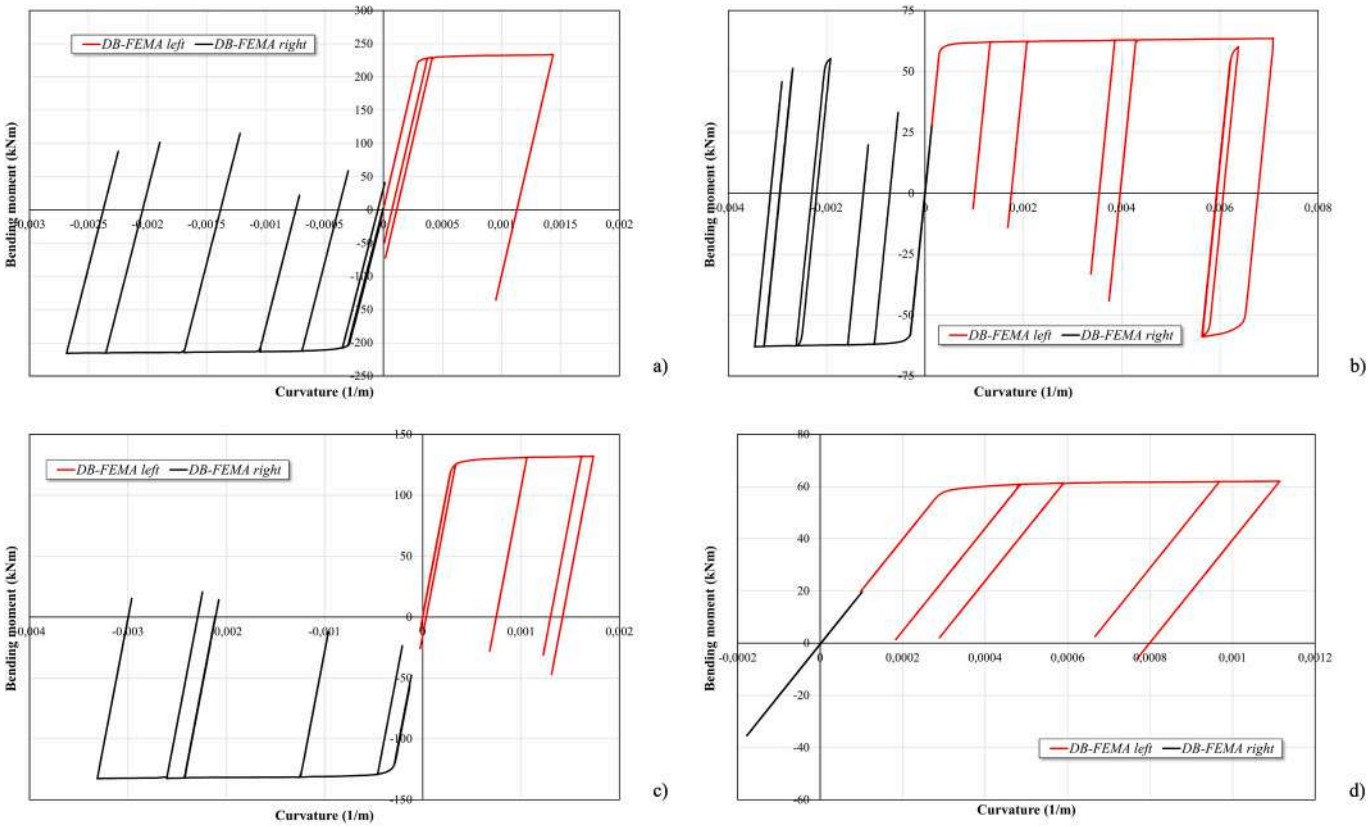

Fig. 24. Bending moment vs curvature: a) beam 7; b) beam 8; c) beam 9; d) beam 10.

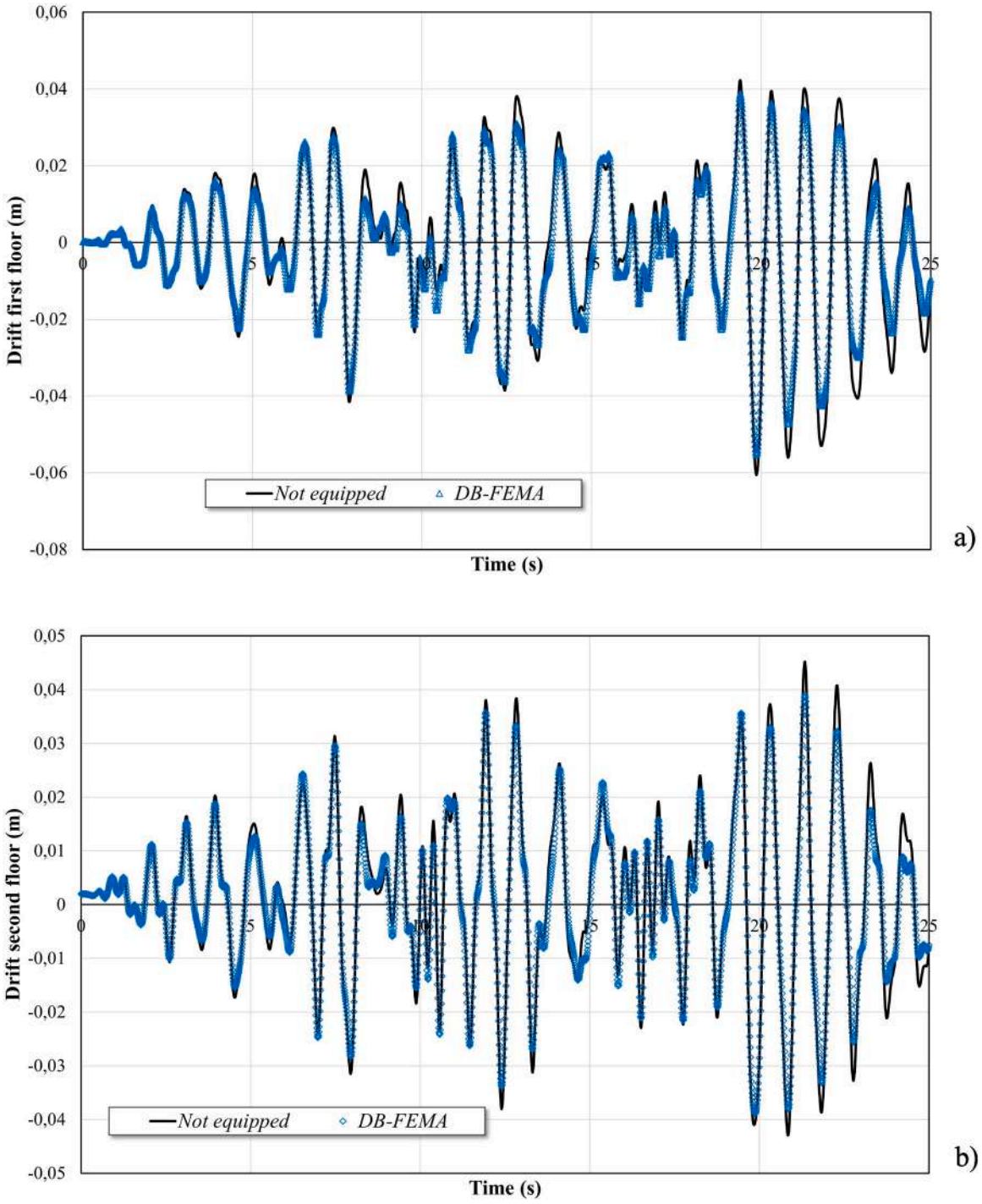

Fig. 25. Drift vs time: a) first floor; b) second floor.

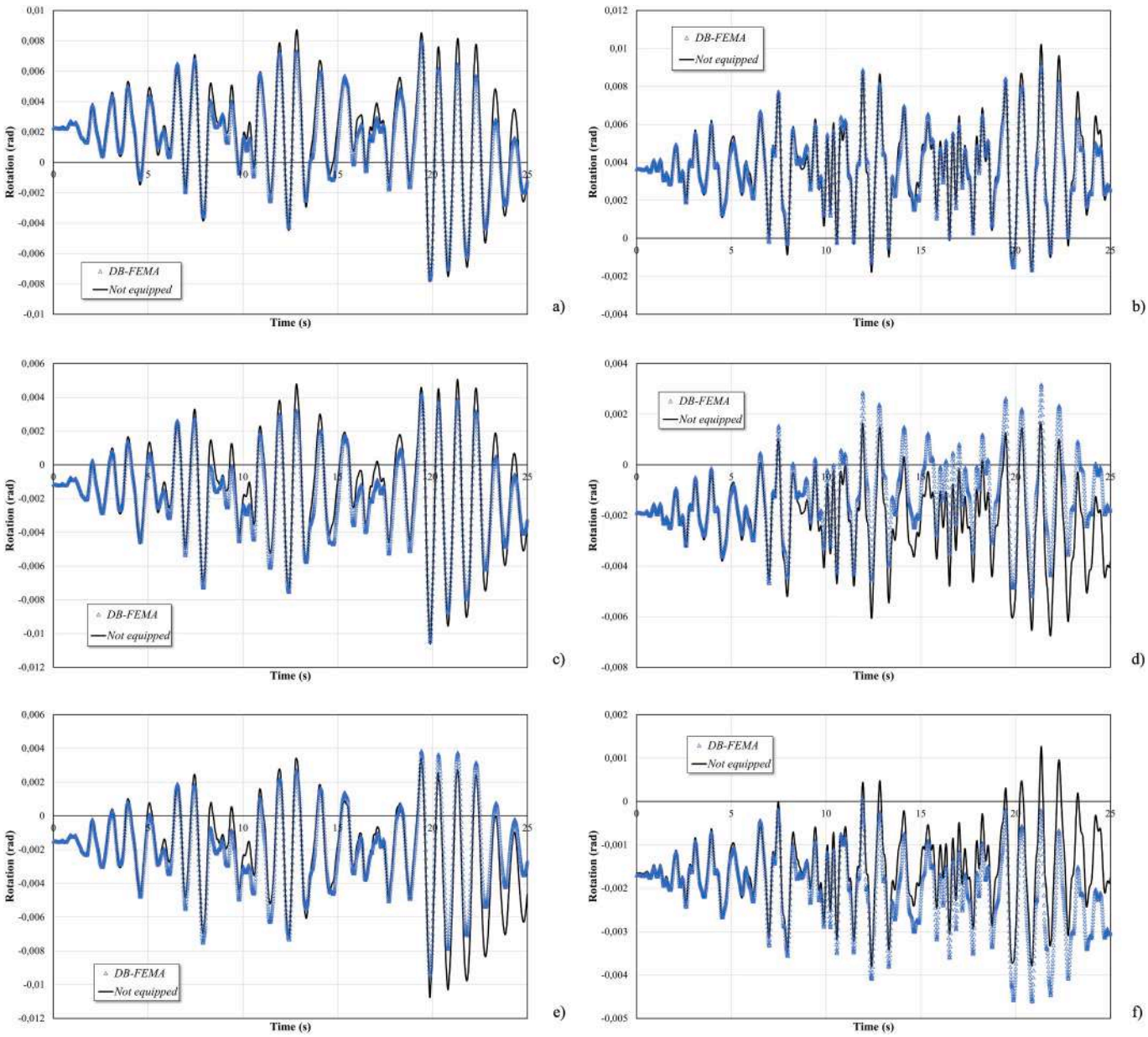

Fig. 26. Rotation vs time: a) Node 2; b) Node 3; c) Node 5; d) Node 6; e) Node 8; f) Node 9.

Table 6
Midspan vertical deflection of the beams in SLE in mm.

Beam	Not equipped	LRPD	Dogbone
7	9.49	9.48	9.61
8	3.36	3.13	3.53
9	12.52	12.52	12.83
10	2.86	2.84	3.07

Declaration of Competing Interest

No funding was received for conducting this study.

The authors have no competing interests to declare that are relevant to the content of this article.

Appendix

In this appendix a synthetic review of the geometrical and mechanical characteristics of the LRPD is reported. LRPD consists of a steel element with suitably assigned features aimed to substitute a portion of a given standard I-shaped steel profile.

In Fig. A.1, the typical standard steel profile is sketched, and its geometry properties are reported in Table A.1.

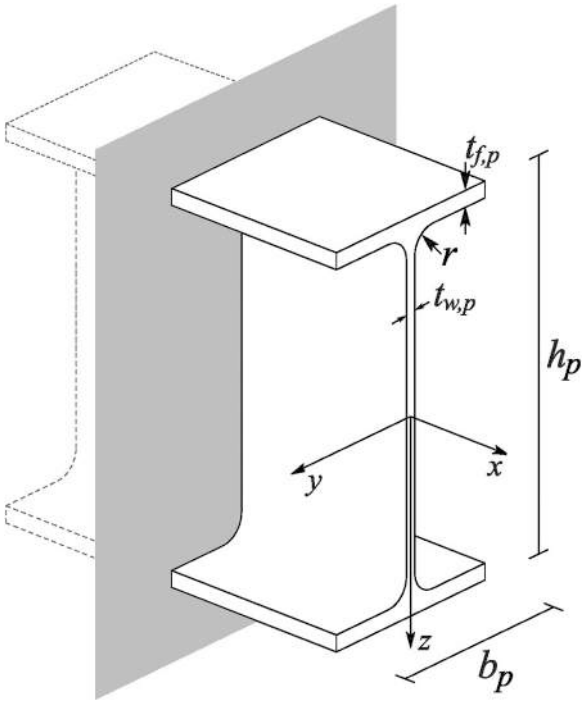

Fig. A.1. Typical standard I-shaped steel profile.

Table A.1
Geometrical characteristics of the standard steel profile.

Adopted Symbol	Description
b_p	Section width
h_p	Section depth
$t_{w,p}$	Web thickness
$t_{f,p}$	Flange thickness
r	Radius

In Figs. A.2-A.3, a scheme of the device is sketched, while in Table A.2 the adopted symbols are reported. As it is possible to observe, the overall device is assumed to be inscribed in a parallelepiped of dimensions $\ell \times b_p \times h_p$.

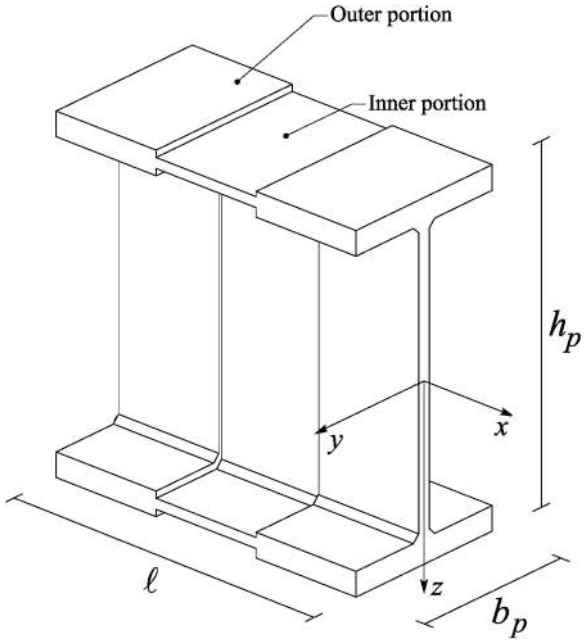

Fig. A.2. Device scheme.

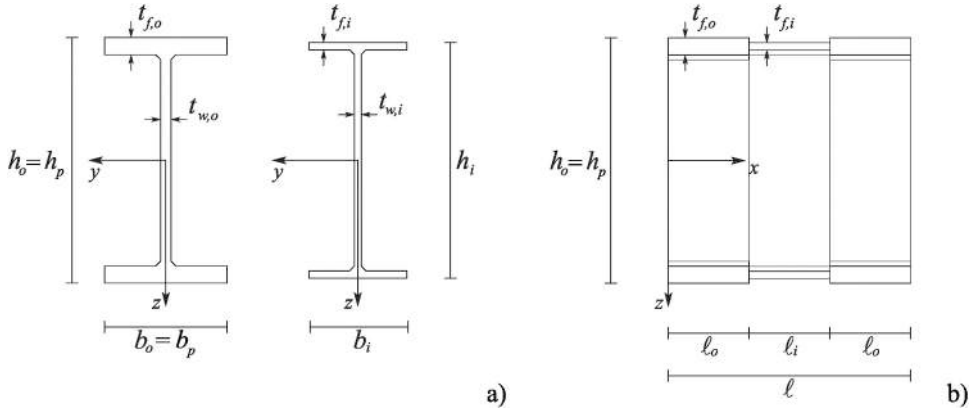

Fig. A.3. Device geometry: a) cross-sections of the outer and inner portions; b) lateral view.

Table A.2
Geometrical characteristics of the device.

Adopted Symbol	Description
Outer portions	
b_o	Section width
h_o	Section depth
$t_{w,o}$	Web thickness
$t_{f,o}$	Flange thickness
ℓ_o	Length
Inner portion	
b_i	Section width
h_i	Section depth
$t_{w,i}$	Web thickness
$t_{f,i}$	Flange thickness
ℓ_i	Length
Overall device	
ℓ	total length
s	welding size

The main geometrical properties of the inner ($k = i$) and outer ($k = o$) cross-section of the LRPD are the following ones:

$$A_k = b_k h_k - \left(b_k - t_{w,k}\right)\left(h_k - 2t_{f,k}\right) \tag{A.1}$$

$$I_k = \frac{b_k h_k^3}{12} - \frac{\left(b_k - t_{w,k}\right)\left(h_k - 2t_{f,k}\right)^3}{12} \tag{A.2}$$

$$W_{el,k} = 2I_k / h_k \tag{A.3}$$

$$W_{pl,k} = \frac{b_k h_k^2}{4} - \frac{\left(b_k - t_{w,k}\right)\left(h_k - 2t_{f,k}\right)^2}{4} \tag{A.4}$$

The main mechanical properties of the inner ($k = i$) and outer ($k = o$) cross-section of the LRPD are related to the definition of the elastic domain (widely treated in Section 2) and of the yield domain. Making reference just to the presence of axial force and of bending moment, and neglecting the influence of the welding sizes, the yield domain boundary (for more details see, [22]) is just constituted by two subsequent portions defined in the following ranges of the neutral axis position (Fig. A.4):

$$0 \le z_n \le \frac{h_k}{2} - t_{f,k} \tag{A.5}$$

if the neutral axis cuts through the web, and

$$\frac{h_k}{2} - t_{f,k} \le z_n \le \frac{h_k}{2} \tag{A.6}$$

if the neutral axis cuts through the flange.

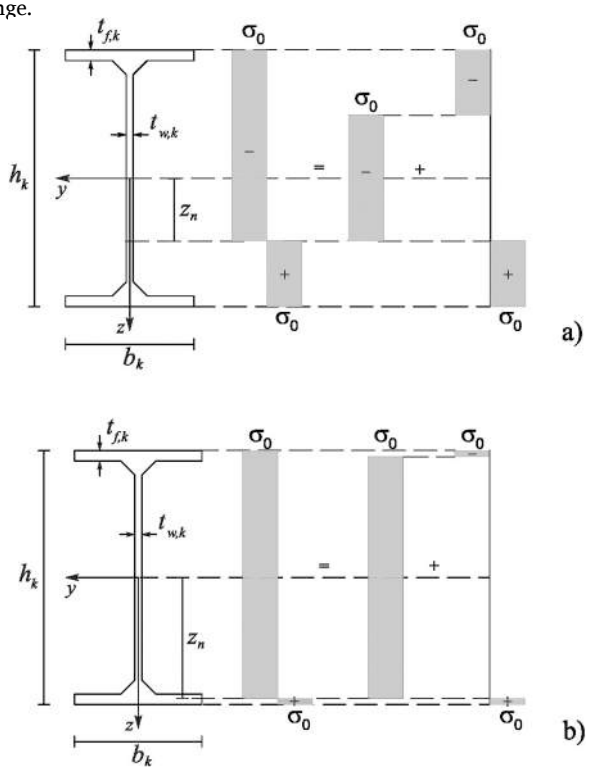

Fig. A.4. Different characteristic ranges of neutral axis positions: a) neutral axis cuts through the web; b) neutral axis cuts through the flange.

.

The locus of a point representing the yield domain boundary for $0 \le z_n \le \frac{h_k}{2} - t_{f,k}$ is provided by the functions

$$N(z_n) = 2t_{w,k} z_n \sigma_0 \tag{A.7}$$

$$M(z_n) = M_{pl,k} - t_{w,k} z_n^2 \sigma_0 \tag{A.8}$$

The locus of a point representing the yield domain boundary for $\frac{h_k}{2} - t_{f,k} \le z_n \le \frac{h_k}{2}$ is provided by the functions

$$N(z_n) = \sigma_0 \left[A_k - 2b_k \left(\frac{h_k}{2} - z_n \right) \right] \tag{A.9}$$

$$M(z_n) = b_k \sigma_0 \left(\frac{h_k^2}{4} - z_n^2 \right) \tag{A.10}$$

In the plane N,M, reducing with respect to z_n, the above reported equations provide the functions $M(N)$ that, with the appropriate substitutions, have the form:

for $0 \le z_n \le \frac{h_k}{2} - t_{f,k}$

$$M = M_{pl,k} - \frac{N^2}{4t_{w,k}\sigma_0} \tag{A.11}$$

for $\frac{h_k}{2} - t_{f,k} \le z_n \le \frac{h_k}{2}$

$$M = \sigma_0\, b_k \left[\frac{{h_k}^2}{4} - \left(\frac{N - \sigma_0 A_k}{2b_k\sigma_0} + \frac{h_k}{2}\right)^2\right] \tag{A.12}$$

The typical yield domain is reported in Fig. A.5.

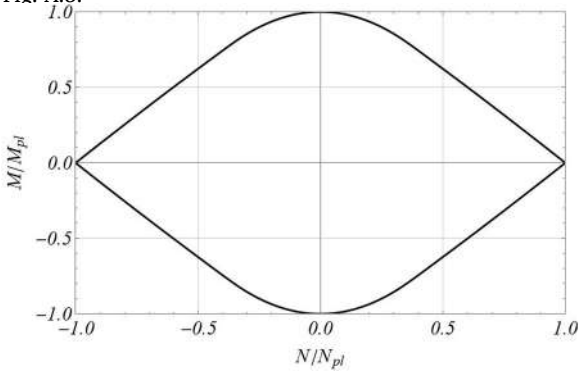

Fig. A5. Typical dimensionless yield domain.

.

References

[1] EN 1993–1-8:2006, Eurocode 3: Design of Steel Structures Part 1–8: Design of Joints, 2006.

[2] Sefcikova K, Brtnik T, Dolejs J, Keltamaki K, Topilla R. Mechanical properties of heat affected zone of high strength steels. IOP Conf Ser: Mater Sci Eng 2015;96: 012053. https://doi.org/10.1088/1757-899X/96/1/012053.

[3] Miller DK. Lessons learned from the Northridge earthquake. Eng Struc 1998;20: 249–60.

[4] Mahin ST. Lessons from damage to steel buildings during the Northridge earthquake. Eng Struct 1998;20(4-6):261–70.

[5] Italian Ministry of Infrastructure and Transport, National Standard NTC 2018, DM 17/01/2018.

[6] Eurocode 8 Design provisions for earthquake resistance of structures, UNI EN 1998–1:2013.

[7] Speicher MS, Harris JL. Collapse prevention seismic performance assessment of new special concentrically braced frames using ASCE 41. 1 November Eng Struct 2016;Volume 126:652–66. https://doi.org/10.1016/j.engstruct.2016.07.064. 1 November.

[8] Faytarouni M, Shen J, Seker O, Akbas B. Evaluation of brace fracture models in seismic analysis of concentrically braced frames. J Constr Steel Res 2019;162: 105709. https://doi.org/10.1016/j.jcsr.2019.105709.

[9] Plumier A. The dogbone: back to the future. Eng J 1997;34:61–7. ISSN 00138029.

[10] Shen J, Kitjasateanphun T, Srivanich W. Seismic performance of steel moment frames with reduced beam sections. Eng Struct 2000;22(8):968–83. https://doi.org/10.1016/S0141-0296(99)00048-6.

[11] Horton TA, Hajirasouliha I, Davison B, Ozdemir Z. More efficient design of reduced beam sections (RBS) for maximum seismic performance. J Constr Steel Res 2021; 183:106728. https://doi.org/10.1016/j.jcsr.2021.106728.

[12] Seismic Performance of Earthquake-Resilient RC Frames Made with HSTC Beams and Friction Damper Devices (2022), Colajanni, Piero; La Mendola, Lidia; Monaco, Alessia; Pagnotta, Salvatore, Journal of Earthquake Engineering, Volume 26, Issue 15, Pages 7787 – 7813, DOI 10.1080/13632469.2021.1964652.

[13] Design of RC joints equipped with hybrid trussed beams and friction dampers, (2021), Colajanni, Piero; La Mendola, Lidia; Monaco, Alessia; Pagnotta, Salvatore, Engineering StructuresVolume 22715 January 2021 Article number 111442, DOI 10.1016/j.engstruct.2020.111442.

[14] Friction-based beam-to-column connection for low-damage RC frames with hybrid trussed beams, (2022), Colajanni, Piero and Pagnotta, Salvatore, Structural Engineering and MechanicsVolume 45, Issue 2, Pages 231 - 24825 October 2022, DOI: 10.12989/scs.2022.45.2.231.

[15] Benfratello S, Palizzolo L. Limited resistance rigid perfectly plastic hinges for steel frames. Intern Rev Civ Eng 2017;8(6):286–98. https://doi.org/10.15866/irece.v8i6.13190.

[16] S. Benfratello, C. Cucchiara, P. Tabbuso, Fixed strength and stiffness hinges for steel frames, in: Feo L., Ascione L., Berardi V.P., Fraternali F., Tralli A.M. (Eds.), AIMETA 2017 – Proc. of the 23rd Conf. of the Italian Association of Theoretical and Applied Mechanics, pp. 1287–1296, ISBN 978–889424847-0.

[17] Benfratello S, Palizzolo L, Tabbuso P, Vazzano S. On the post elastic behavior of LRPH connections. Int Rev Model Simul 2019;12:341–53. https://doi.org/10.15866/iremos.v12i6.18294.

[18] L. Palizzolo, S. Benfratello, P. Tabbuso, S. Vazzano, Numerical validation of LRPH behaviour by fem analysis, Advances in Engineering Materials, Structures and Systems: Innovations, Mechanics and Applications - Proceedings of the 7th International Conference on Structural Engineering, Mechanics and Computation, 2019, 2019, 1224–1229, DOI 10.1201/9780429426506–212.

[19] Benfratello S, Palizzolo L, Tabbuso P, Vazzano S. LRPH device optimization for axial and shear stresses. Intern Rev Civ Eng 2020;11(4):152–63. https://doi.org/10.15866/irece.v11i4.18100.

[20] S. Benfratello, S. Caddemi, L. Palizzolo, B. Pantò, D. Rapicavoli, S. Vazzano, Smart beam element approach for lrph device, in: Carcaterra A., Graziani G., Paolone A. (Eds), 24th Conference of the Italian Association of Theoretical and Applied Mechanics, AIMETA 2019, Lecture Notes in Mechanical Engineering (2020), 197–213, DOI 10.1007/978–3-030–41057-5_16.

[21] Benfratello S, Caddemi S, Palizzolo L, Pantò B, Rapicavoli D, Vazzano S. Targeted steel frames by means of innovative moment resisting connections. J Constr Steel Res 2021;183:106695. https://doi.org/10.1016/j.jcsr.2021.106695.

[22] Benfratello S, Palizzolo L, Vazzano S. A New Design Problem in the Formulation of a Special Moment Resisting Connection Device for Preventing Local Buckling. J Appl Sci 2022;12:202. https://doi.org/10.3390/app12010202.

[23] Saleh A, Mirghaderi SR, Zahrai SM. Cyclic testing of tubular web RBS connections in deep beams. J Constr Steel Res 2016;117:214–26. https://doi.org/10.1016/j.jcsr.2015.10.020.

[24] Momenzadeh S, Kazemi MT, Asl MH. Seismic performance of reduced web section moment connections. Int J Steel Struct 2017;17(2):413–25. https://doi.org/10.1007/s13296-017-6004-x.

[25] Tabar AM, Alonso-Rodriguez A, Tsavdaridis KD. Building retrofit with reduced web (RWS) and beam (RBS) section limited-ductility connections. J Constr Steel Res 2022;197:107459. https://doi.org/10.1016/j.jcsr.2022.107459.

[26] Saeedi H, Erfani S. Cyclic behavior of a novel bolted beam-to-box column connection with reduced beam section. Structures 2023;53:1369–88. https://doi.org/10.1016/j.istruc.2023.05.016.

[27] AISC 2016, Prequalified connections for special and intermediate steel moment frames for seismic applications. ANSI/AISC 358–16. Chicago.

[28] FEMA-350, Recommended seismic design criteria for new steel moment-frame buildings, 2000, Federal Emergency Management Agency.

[29] AS 4100–1998l; Australian Standard: Steel Structures. STANDARDS AUSTRALIA: Sydney, SA, Australia, 2012.

[30] Goczek J, Supeł Ł. Resistance of steel cross-sections subjected to bending, shear and axial forces. Eng Struct 2014;70:271–7. https://doi.org/10.1016/j.engstruct.2014.02.016.

[31] Gusella F, Orlando M, Peterman KD. The impact of variability and combined loads on fuses in braced frames. Structures 2022;35:650–66. https://doi.org/10.1016/j.istruc.2021.11.027.